Supporting Information

Table S1: Flow cytometry labeling conditions.

Detection	Primary label (dilution)	Secondary label (dilution)
HA tag (displaying)	Mouse anti-HA (1:500)	Goat anti-mouse Alexa Fluor 488 (1:500)
c-Myc tag (full length)	Chicken anti-CMYC (1:500)	Goat anti-chicken Alexa Fluor 647 (1:500)

Table S2: Relative readthrough efficiency error as a percentage of the RRE magnitude for three reporter systems (yeast display, RFP-GFP dual-fluorescent protein reporter, sfGFP single-fluorescent protein reporter).

	Detection Method	LeuOmeRS + OmeY	LeuOmeRS + AzF	TyrOmeRS + OmeY	TyrOmeRS + AzF
Yeast Display	Flow Cytometry	13%	15%	17%	9.9%
RFP/GFP	Flow Cytometry	5.6%	5.3%	19%	19%
GFP	Flow Cytometry	10%	2.3%	16%	15%
RFP/GFP	Plate Reader	20%	40%	20%	21%
GFP	Plate Reader	19%	140%	22%	19%

Table S3: Relative readthrough efficiency error as a percentage of the RRE magnitude for various dual-fluorescent protein reporters.

	Detection Method	LeuOmeRS + OmeY	LeuOmeRS + AzF	TyrOmeRS + OmeY	TyrOmeRS + AzF
RFP/GFP	Flow Cytometry	5.6%	5.3%	19%	19%
BFP/GFP	Flow Cytometry	15%	13%	7.6%	7.5%
GFP/BFP	Flow Cytometry	43%	40%	32%	28%
RFP/GFP	Plate Reader	20%	40%	20%	21%
BFP/GFP	Plate Reader	21%	24%	23%	16%
GFP/BFP	Plate Reader	37%	210%	76%	73%

Table S4: One-way ANOVA with groupings via the Games-Howell method to evaluate the abilities of yeast display, RFP-GFP, and sfGFP reporters to discriminate between ncAA incorporation events of varying efficiencies (and wild-type controls) via flow cytometer.

				Flow Cytometry Data											
				Yeast Display				RFP-GFP				GFP			
				N	Mean	95% CI	Grouping	N	Mean	95% CI	Grouping	N	Mean	95% CI	Grouping
N-terminal Detection	Wild-type	LeuOmeRS	none	3	1387.4	(1245.0, 1529.9)	B	3	989.7	(899.0, 1080.3)	A B				
			OmeY	3	1482.4	(1259.5, 1705.2)	B	3	1057.4	(1007.5, 1107.2)	A				
			AzF	3	1478.7	(1212.4, 1744.9)	B	3	1065.03	(1030.13, 1099.94)	A				
		TyrOmeRS	none	3	1490.1	(1399.0, 1581.2)	B	3	935	(829.8, 1040.2)	A B				
			OmeY	3	1455	(1222.8, 1687.3)	B	3	1000	(984.49, 1015.51)	A B				
			AzF	3	1561.3	(1421.1, 1701.6)	B	3	1131.3	(1001.2, 1261.5)	A				
	TAG construct	LeuOmeRS	none	3	1957.8	(1858.6, 2057.0)	A B	3	769.7	(682.7, 856.7)	B				
			OmeY	3	2048	(1807.8, 2288.2)	A	3	1073.4	(952.7, 1194.1)	A				
			AzF	3	1980.1	(1586.1, 2374.1)	A B	3	905.6	(838.3, 973.0)	A B				
		TyrOmeRS	none	3	1910.8	(1786.5, 2035.0)	A B	3	736.3	(659.3, 813.4)	B				
			OmeY	3	1999	(1259, 2738)	A B	3	947.4	(809.5, 1085.3)	A B				
			AzF	3	2000.4	(1602.3, 2398.5)	A B	3	1043.4	(836.9, 1249.9)	A B				
C-terminal Detection	Wild-type	LeuOmeRS	none	3	37313	(33179, 41448)	A	3	6130	(5117, 7144)	A B	3	26298	(21618, 30979)	A
			OmeY	3	35888	(29681, 42094)	A	3	6387.7	(6234.1, 6541.4)	A	3	23944	(20320, 27568)	A
			AzF	3	33012	(29357, 36667)	A	3	6567	(5895, 7240)	A	3	25777	(24503, 27051)	A
		TyrOmeRS	none	3	32599	(30400, 34798)	A	3	5961	(5074, 6848)	A B	3	27279	(20285, 34272)	A
			OmeY	3	34140	(29721, 38560)	A	3	6283	(5866.1, 6699.9)	A	3	22298	(15125, 29471)	A
			AzF	3	34697	(31573, 37821)	A	3	6708	(5759, 7657)	A	3	26485	(18567, 34404)	A
	TAG construct	LeuOmeRS	none	3	286.7	(239.4, 334.0)	F	3	81.63	(75.97, 87.30)	E	3	889.3	(711.2, 1067.5)	D
			OmeY	3	16375	(13417, 19333)	B	3	4164.7	(3894.5, 4435.0)	B C	3	5439	(4317, 6561)	B
			AzF	3	1051.3	(794.6, 1308.1)	C	3	442.67	(434.91, 450.42)	D E	3	989	(957.87, 1020.13)	D
		TyrOmeRS	none	3	364.7	(337.11, 392.29)	F	3	132.37	(98.69, 166.05)	E	3	1235.7	(999.6, 1471.8)	D
			OmeY	3	5269.3	(4844.2, 5694.4)	D	3	2398	(1346, 3450)	C D E	3	2782	(2180, 3384)	C
			AzF	3	7211	(6701, 7722)	E	3	2742	(1698, 3785)	C D	3	3176	(2535, 3818)	C

**Means that do not share a letter are statistically different*

Table S5: One-way ANOVA with groupings via the Games-Howell method to evaluate the abilities of RFP-GFP, and sfGFP reporters to discriminate between ncAA incorporation events of varying efficiencies (and wild-type controls) via microplate reader.

				Microplate Reader Data							
				RFP-GFP				GFP			
				N	Mean	95% CI	Grouping	N	Mean	95% CI	Grouping
N-terminal Detection	Wild-type	LeuOmeRS	none	3	620515	(495173, 745857)	A B				
			OmeY	3	641626	(540257, 742996)	A				
			AzF	3	599362	(572771, 625954)	A B				
		TyrOmeRS	none	3	604032	(493554, 714509)	A B				
			OmeY	3	551924	(465708, 638139)	A B				
			AzF	3	562679	(459852, 665507)	A B				
	TAG construct	LeuOmeRS	none	3	448974	(407652, 490296)	A B				
			OmeY	3	536657	(499394, 573920)	A B				
			AzF	3	416156	(368893, 463418)	B				
		TyrOmeRS	none	3	408299	(342151, 474448)	B				
			OmeY	3	456924	(399847, 514000)	B				
			AzF	3	510425	(440547, 580303)	A B				
C-terminal Detection	Wild-type	LeuOmeRS	none	3	12391834	(9043994, 15739675)	A	3	24060972	(18929613, 29192331)	A
			OmeY	3	11578707	(8755388, 14402026)	A	3	21723180	(15872683, 27573676)	A
			AzF	3	11362153	(10072694, 12651611)	A	3	22826754	(19084945, 26568563)	A
		TyrOmeRS	none	3	11068101	(9600508, 12535694)	A	3	23105251	(17436634, 28773869)	A
			OmeY	3	9827196	(8133696, 11520696)	A	3	19059034	(14429691, 23688377)	A
			AzF	3	10088130	(7772110, 12404150)	A	3	20887844	(14552549, 27223139)	A
	TAG construct	LeuOmeRS	none	3	60903	(-584984, 706790)	C	3	200056	(-472961, 873073)	C
			OmeY	3	7974976	(6850592, 9099361)	A	3	4018956	(2379751, 5658161)	B
			AzF	3	822572	(116018, 1529127)	C	3	218640	(-574756, 1012035)	C
		TyrOmeRS	none	3	539344	(-528534, 1607221)	C	3	236415	(-853429, 1326258)	C
			OmeY	3	4632104	(3744436, 5519773)	B	3	1852495	(589714, 3115277)	B C
			AzF	3	5688804	(4815829, 6561779)	A B	3	2348903	(1061853, 3635953)	B C

**Means that do not share a letter are statistically different*

Table S6: One-way ANOVA with groupings via the Games-Howell method to evaluate the abilities of RFP-GFP, BFP-GFP, and GFP-BFP reporters to discriminate between ncAA incorporation events of varying efficiencies (and wild-type controls) via flow cytometry.

				Flow Cytometry Data											
				RFP-GFP				BFP-GFP				GFP-BFP			
				N	Mean	95% CI	Grouping	N	Mean	95% CI	Grouping	N	Mean	95% CI	Grouping
N-terminal Detection	Wild-type	LeuOmeRS	none	3	989.7	(899.0, 1080.3)	A B	3	8453	(7561, 9344)	D	3	23632	(16754, 30511)	A
			OmeY	3	1057.4	(1007.5, 1107.2)	A	3	9834	(9239, 10430)	C D	3	24920	(16531, 33310)	A
			AzF	3	1065.03	(1030.13, 1099.94)	A	3	10832	(9780, 11883)	B C D	3	26129	(19447, 32811)	A
		TyrOmeRS	none	3	935	(829.8, 1040.2)	A B	3	9321	(8129, 10513)	D	3	23859	(16159, 31558)	A
			OmeY	3	1000	(984.49, 1015.51)	A B	3	9838	(9414.9, 10261.1)	C D	3	24344	(15180, 33508)	A
			AzF	3	1131.3	(1001.2, 1261.5)	A	3	11855	(10687, 13022)	A B C	3	26838	(14979, 38697)	A
	TAG construct	LeuOmeRS	none	3	769.7	(682.7, 856.7)	B	3	7928	(7164, 8692)	D	3	13485	(4711, 22259)	A
			OmeY	3	1073.4	(952.7, 1194.1)	A	3	11503	(8443, 14564)	A B C D	3	21830	(8365, 35295)	A
			AzF	3	905.6	(838.3, 973.0)	A B	3	11293	(9429, 13158)	A B C D	3	15487	(5238, 25735)	A
		TyrOmeRS	none	3	736.3	(659.3, 813.4)	B	3	9239	(7961, 10518)	D	3	14220	(11462, 16977)	A
			OmeY	3	947.4	(809.5, 1085.3)	A B	3	12459	(11870, 13048)	A B	3	17990	(11661, 24319)	A
			AzF	3	1043.4	(836.9, 1249.9)	A B	3	13509	(12608, 14410)	A	3	22706	(18576, 26836)	A
C-terminal Detection	Wild-type	LeuOmeRS	none	3	6130	(5117, 7144)	A B	3	10373	(9264, 11481)	C D	3	26409	(17137, 35682)	A
			OmeY	3	6387.7	(6234.1, 6541.4)	A	3	12425	(11980, 12870)	A B C	3	28690	(16785, 40595)	A
			AzF	3	6567	(5895, 7240)	A	3	13463	(12322, 14603)	A B	3	29783	(21053, 38512)	A
		TyrOmeRS	none	3	5961	(5074, 6848)	A B	3	11812	(10432, 13192)	B C	3	27057	(18320, 35794)	A
			OmeY	3	6283	(5866.1, 6699.9)	A	3	12457	(11927, 12987)	A B	3	27824	(16820, 38828)	A
			AzF	3	6708	(5759, 7657)	A	3	15115	(13764, 16466)	A	3	30569	(17001, 44136)	A
	TAG construct	LeuOmeRS	none	3	81.63	(75.97, 87.30)	E	3	67.67	(59.08, 76.25)	H	3	248.3	(78.2, 418.5)	A
			OmeY	3	4164.7	(3894.5, 4435.0)	B C	3	7625	(5776, 9474)	D E	3	8668	(2790, 14546)	A
			AzF	3	442.67	(434.91, 450.42)	D E	3	721.8	(550.2, 893.3)	F	3	537	(197.1, 876.9)	A
		TyrOmeRS	none	3	132.37	(98.69, 166.05)	E	3	118.07	(109.53, 126.60)	G	3	373	(341.87, 404.13)	A
			OmeY	3	2398	(1346, 3450)	C D E	3	4262	(3531, 4993)	E	3	3544	(1921, 5167)	A
			AzF	3	2742	(1698, 3785)	C D	3	5370	(4764, 5976)	E	3	5189	(3970, 6407)	A

**Means that do not share a letter are statistically different*

Table S7: One-way ANOVA with groupings via the Games-Howell method to evaluate the reproducibility of GFP-BFP reporter performance via flow cytometry.

				Flow Cytometry Data (Reproduced)			
				GFP-BFP			
				N	Mean	95% CI	Grouping
N-terminal Detection	Wild-type	LeuOmeRS	none	3	26344	(18397, 34292)	A B
			OmeY	3	22921	(16210, 29631)	A B
			AzF	3	28675	(20598, 36752)	A
		TyrOmeRS	none	3	27610	(18311, 36909)	A B
			OmeY	3	21320	(14482, 28158)	A B
			AzF	3	26979	(15720, 38238)	A B
	TAG construct	LeuOmeRS	none	3	14585	(5345, 23826)	A B
			OmeY	3	22040	(7072, 37009)	A B
			AzF	3	17315	(6307, 28323)	A B
		TyrOmeRS	none	3	14372	(8887, 19857)	B
			OmeY	3	16170	(11584, 20757)	A B
			AzF	3	20171	(13699, 26643)	A B
C-terminal Detection	Wild-type	LeuOmeRS	none	3	28140	(17329, 38950)	A
			OmeY	3	25217	(16396, 34038)	A B
			AzF	3	30921	(21265, 40578)	A
		TyrOmeRS	none	3	30120	(20438, 39801)	A B
			OmeY	3	23831	(16921, 30741)	A B
			AzF	3	29901	(17745, 42057)	A B
	TAG construct	LeuOmeRS	none	3	280.7	(38.7, 522.6)	C
			OmeY	3	9617	(955, 18279)	B C
			AzF	3	640	(198, 1082)	B C
		TyrOmeRS	none	3	406.7	(246.4, 566.9)	C
			OmeY	3	3387	(1558, 5217)	B C
			AzF	3	4814	(1778, 7858	B C

**Means that do not share a letter are statistically different*

Table S8: One-way ANOVA with groupings via the Games-Howell method to evaluate the abilities of RFP-GFP, BFP-GFP, and GFP-BFP reporters to discriminate between ncAA incorporation events of varying efficiencies (and wild-type controls) via microplate reader.

				Microplate Reader Data											
				RFP-GFP				BFP-GFP				GFP-BFP			
				N	Mean	95% CI	Grouping	N	Mean	95% CI	Grouping	N	Mean	95% CI	Grouping
N-terminal Detection	Wild-type	LeuOmeRS	none	3	620515	(495173, 745857)	A B	3	10706239	(9752387, 11660091)	A	3	23540322	(16520045, 30560599)	A
			OmeY	3	641626	(540257, 742996)	A	3	9465516	(7432078, 11498954)	A	3	20651655	(15130827, 26172483)	A
			AzF	3	599362	(572771, 625954)	A B	3	10359836	(10059445, 10660226)	A	3	23771617	(16215718, 31327516)	A
		TyrOmeRS	none	3	604032	(493554, 714509)	A B	3	9462927	(7113018, 11812837)	A	3	22105138	(16745600, 27464676)	A
			OmeY	3	551924	(465708, 638139)	A B	3	8713931	(7409970, 10017892)	A	3	17089913	(12041813, 22138014)	A
			AzF	3	562679	(459852, 665507)	A B	3	10377311	(9403552, 11351069)	A	3	20376906	(14440720, 26313092)	A
	TAG construct	LeuOmeRS	none	3	448974	(407652, 490296)	A B	3	10394040	(9394451, 11393629)	A	3	12494469	(3993947, 20994991)	A
			OmeY	3	536657	(499394, 573920)	A B	3	9012477	(7689337, 10335617)	A	3	16670226	(10682510, 22657942)	A
			AzF	3	416156	(368893, 463418)	B	3	10568754	(7730818, 13406689)	A	3	13538609	(5128754, 21948464)	A
		TyrOmeRS	none	3	408299	(342151, 474448)	B	3	12620939	(10422772, 14819105)	A	3	12420048	(10639622, 14200474)	A
			OmeY	3	456924	(399847, 514000)	B	3	11164627	(7953631, 14375624)	A	3	14311679	(9829997, 18793361)	A
			AzF	3	510425	(440547, 580303)	A B	3	13538616	(10504511, 16572720)	A	3	15777682	(12070723, 19484641)	A
C-terminal Detection	Wild-type	LeuOmeRS	none	3	12391834	(9043994, 15739675)	A	3	29926249	(23143138, 36709359)	A	3	7755078	(4678883, 10831273)	A
			OmeY	3	11578707	(8755388, 14402026)	A	3	24820691	(17492926, 32148456)	A B C	3	7444236	(4082222, 10806249)	A B
			AzF	3	11362153	(10072694, 12651611)	A	3	28910583	(24958136, 32863030)	A	3	7703980	(3707880, 11700080)	A B
		TyrOmeRS	none	3	11068101	(9600508, 12535694)	A	3	25228671	(18846129, 31611212)	A B	3	7315088	(5959395, 8670781)	A B
			OmeY	3	9827196	(8133696, 11520696)	A	3	23068601	(18084324, 28052878)	A B C	3	6022844	(3593073, 8452614)	A B
			AzF	3	10088130	(7772110, 12404150)	A	3	29334925	(24602574, 34067275)	A	3	6928395	(5272844, 8583946)	A B
	TAG construct	LeuOmeRS	none	3	60903	(-584984, 706790)	C	3	65172	(-605078, 735422)	E	3	-337784	(-1978503, 1302934)	C
			OmeY	3	7974976	(6850592, 9099361)	A	3	14015849	(13021805, 15009893)	B C	3	2680573	(-113144, 5474290)	A B C
			AzF	3	822572	(116018, 1529127)	C	3	1599123	(886230, 2312017)	D	3	-347913	(-2411930, 1716103)	C
		TyrOmeRS	none	3	539344	(-528534, 1607221)	C	3	834882	(-188738, 1858502)	D E	3	-349264	(-3289472, 2590944)	C
			OmeY	3	4632104	(3744436, 5519773)	B	3	11426749	(9123118, 13730380)	C	3	1664856	(-1183091, 4512802)	B C
			AzF	3	5688804	(4815829, 6561779)	A B	3	15241406	(12980846, 17501966)	B C	3	1350448	(-787925, 3488820)	B C

**Means that do not share a letter are statistically different*

Table S9: One-way ANOVA with groupings via the Games-Howell method to evaluate the extent to which BFP-GFP reporters (BXG, AltTAG, AltTAG2, AltTAG3, AltTAG4 and 2TAG) support statistically distinct levels of readthrough efficiency via flow cytometry.

			Flow Cytometry Data							
			LeuOmeRS				TyrOmeRS			
			N	Mean	95% CI	Grouping	N	Mean	95% CI	Grouping
No ncAA	N-terminal Detection	BYG	3	35410	(28853, 41966)	A	3	36976	(25386, 48566)	A
		BXG	3	32982	(30406, 35557)	A	3	34838	(32898, 36778)	A
		AltTAG	3	32253	(23368, 41138)	A	3	32674	(27699, 37648)	A
		AltTAG2	3	29952	(20449, 39454)	A	3	34036	(16091, 51981)	A
		AltTAG3	3	35486	(33197, 37775)	A	3	35193	(34398, 35987)	A
		AltTAG4	3	28782	(27938, 29626)	A	3	31288	(26073, 36503)	A
		2TAG	3	35734	(16441, 55026)	A	3	31198	(10004, 52391)	A
	C-terminal Detection	BYG	3	31684	(25184, 38185)	A	3	31773	(19448, 44097)	A
		BXG	3	185	(169.49, 200.51)	B	3	293	(233.4, 352.6)	B
		AltTAG	3	47.67	(35.93, 59.41)	D	3	94.3	(36.1, 152.6)	C D
		AltTAG2	3	46	(39.43, 52.57)	D	3	107.7	(56.5, 158.8)	C D
		AltTAG3	3	74.67	(68.42, 80.92)	C	3	135	(93.96, 176.04)	C
		AltTAG4	3	48.33	(33.78, 62.89)	D	3	88.67	(73.49, 103.84)	C D
		2TAG	3	23	(-3.29, 49.29	D	3	38	(10.01, 65.99)	D
OmeY	N-terminal Detection	BYG	3	29430	(17375, 41485)	A	3	30031	(17723, 42338)	A
		BXG	3	33571	(24603, 42539)	A	3	37602	(22552, 52653)	A
		AltTAG	3	36803	(27473, 46133)	A	3	36408	(24832, 47985)	A
		AltTAG2	3	23112	(13957, 32266)	A	3	23644	(8904, 38383)	A
		AltTAG3	3	35684	(15805, 55563)	A	3	28243	(331, 56156)	A
		AltTAG4	3	34288	(25401, 43175)	A	3	36803	(17590, 56016)	A
		2TAG	3	51350	(28332, 74369)	A	3	39453	(36987, 41920)	A
	C-terminal Detection	BYG	3	25853	(14719, 36987)	A	3	26186	(13388, 38984)	A
		BXG	3	14699	(9869, 19528)	A	3	9237	(3810, 14664)	A
		AltTAG	3	3835	(2985, 4684)	A B	3	1940	(525, 3355)	A
		AltTAG2	3	2118	(1201, 3035)	B	3	1208	(327, 2089)	A
		AltTAG3	3	5580	(1631, 9530)	B	3	1782	(-300, 3865)	A
		AltTAG4	3	1873	(669, 3077)	B	3	1473	(528, 2419)	A
		2TAG	3	3130	(1853, 4407)	B	3	593	(498.5, 687.5)	A
AzF	N-terminal Detection	BYG	3	39138	(34517, 43758)	A	3	37525	(28872, 46179)	A
		BXG	3	41435	(40534, 42336)	A	3	45489	(42796, 48182)	A
		AltTAG	3	22375	(18923, 25827)	A	3	24541	(-721, 49803)	A
		AltTAG2	3	22286	(19577, 24995)	A	3	25846	(258, 51434)	A
		AltTAG3	3	42395	(28499, 56291)	A	3	48993	(38879, 59108)	A
		AltTAG4	3	35931	(28629, 43234)	A	3	43624	(38284, 48963)	A
		2TAG	3	44608	(27757, 61459)	A	3	43144	(42011, 44277)	A
	C-terminal Detection	BYG	3	35625	(31667, 39583)	A	3	33520	(25299, 41741)	A
		BXG	3	1475.7	(1298.4, 1652.9)	B	3	12357	(11299, 13415)	B
		AltTAG	3	137	(108.79, 165.21)	C	3	1277	(-208, 2762)	C
		AltTAG2	3	128.33	(114.21, 142.46)	C	3	1492	(-626, 3609	C
		AltTAG3	3	297.3	(180.4, 414.2)	C	3	3763	(1513, 6012)	C
		AltTAG4	3	113.67	(95.02, 132.31)	C	3	1923	(1483, 2363)	C
		2TAG	3	46.67	(17.66, 75.67)	D	3	761.7	(686.4, 836.9)	C

**Means that do not share a letter are statistically different*

Table S10: One-way ANOVA with groupings via the Games-Howell method to evaluate the varying expression levels of N-terminal detection for the alternate BFP-GFP reporter (AltTAG) with various BY4741 single gene knockout strains via flow cytometry.

			Flow Cytometry Data: BFP-GFP (AltTAG)							
			LeuOmeRS				TyrOmeRS			
			N	Mean	95% CI	Grouping	N	Mean	95% CI	Grouping
No ncAA	N-terminal Detection	BY4741	3	20239	(19287, 21190)	B	3	19346	(17190, 21502)	C
		ΔUPF1	3	40479	(37804, 43154)	A	3	38690	(37595, 39786)	A
		ΔUPF2	3	39594	(36600, 42588)	A	3	33113	(29700, 36526)	A B
		ΔUPF3	3	40374	(36251, 44497)	A	3	33305	(29718, 36893)	A B
		ΔTPA1	3	21897	(19478, 24316)	B	3	20437	(17900, 22975)	C
		ΔPOP2	3	24063	(20822, 27305)	B	3	21875	(19179, 24572)	C
		ΔPPQ1	3	24012	(21109, 26915)	B	3	30654	(27219, 34089)	B
OmeY	N-terminal Detection	BY4741	3	23193	(21566, 24819)	B	3	22976	(19225, 26727)	E
		ΔUPF1	3	36904	(35454, 38354)	A	3	37447	(35215, 39679)	B
		ΔUPF2	3	33000	(25865, 40136)	A B	3	32290	(30556, 34024)	C
		ΔUPF3	3	34451	(31500, 37403)	A	3	30343	(27617, 33069)	C D
		ΔTPA1	3	28704	(26088, 31321)	B	3	28496	(27016, 29977)	D E
		ΔPOP2	3	28452	(22806, 34098)	A B	3	30567	(26390, 34744)	C D
		ΔPPQ1	3	34090	(24392, 43787)	A B	3	45845	(45069, 46621)	A
AzF	N-terminal Detection	BY4741	3	20931	(19306, 22557)	B	3	25622.7	(25370, 25875.3)	C
		ΔUPF1	3	40284	(31910, 48657)	A	3	36715	(31307, 42123)	A B
		ΔUPF2	3	40705	(33263, 48147)	A	3	33747	(32825, 34669)	B
		ΔUPF3	3	40226	(38691, 41760)	A	3	32040	(29326, 34754)	B
		ΔTPA1	3	23228	(20242, 26213)	B	3	30653	(29433, 31873)	B
		ΔPOP2	3	24579	(21869, 27288)	B	3	30078	(23062, 37095)	B C
		ΔPPQ1	3	25138	(20239, 30038)	B	3	46198	(45283, 47112)	A
*Means that do not share a letter are statistically different										

Table S11: One-way ANOVA with groupings via the Games-Howell method to evaluate the varying expression levels of N-terminal detection for the BFP-GFP reporter (BXG) with various BY4741 single gene knockout strains via flow cytometry.

			Flow Cytometry Data: BFP-GFP (BXG)							
			LeuOmeRS				TyrOmeRS			
			N	Mean	95% CI	Grouping	N	Mean	95% CI	Grouping
No ncAA	N-terminal Detection	BY4741	3	21842	(20519, 23165)	C	3	22214	(19782, 24646)	B
		ΔUPF1	3	40239	(35152, 45327)	A	3	24240	(-24791, 73271)	A B
		ΔUPF2	3	40741	(36537, 44945)	A	3	31581	(26703, 36458)	A
		ΔUPF3	3	39293	(34245, 44342)	A	3	28729	(11789, 45669)	A B
		ΔTPA1	3	24866	(20806, 28927)	B C	3	22237	(19672, 24802)	B
		ΔPOP2	3	25093	(22536, 27651)	B C	3	24151	(22582, 25720)	A B
		ΔPPQ1	3	27321	(24066, 30577)	B	3	30158	(26379, 33936)	A
OmeY	N-terminal Detection	BY4741	3	25217	(24785, 25650)	B	3	26170	(23077, 29262)	B
		ΔUPF1	3	30181	(28558, 31804)	B	3	20145	(-20097, 60387)	A B
		ΔUPF2	3	26703	(23716, 29689)	B	3	25476	(23820, 27132)	B
		ΔUPF3	3	27402	(25485, 29319)	B	3	23226	(11752, 34700)	A B
		ΔTPA1	3	30667	(23963, 37371)	A B	3	29182	(27342, 31022)	B
		ΔPOP2	3	29854	(28143, 31565)	B	3	30352	(26227, 34478)	B
		ΔPPQ1	3	37452	(34579, 40325)	A	3	39512	(34341, 44683)	A
AzF	N-terminal Detection	BY4741	3	22982	(20118, 25846)	C	3	27806	(26300, 29312)	C D
		ΔUPF1	3	38289	(36302, 40277)	A	3	19546	(-19395, 58487)	A B C D
		ΔUPF2	3	37314	(29370, 45259)	A B	3	26292	(24915, 27669)	D
		ΔUPF3	3	38267	(34937, 41596)	A	3	24433	(12446, 36420)	A B C D
		ΔTPA1	3	25831	(22826, 28836)	B C	3	30374	(28048, 32701)	B C
		ΔPOP2	3	26434	(25195, 27672)	B C	3	32514	(31093, 33936)	B
		ΔPPQ1	3	29695	(26503, 32886)	B	3	40822	(36337, 45307)	A

**Means that do not share a letter are statistically different*

Table S12: One-way ANOVA with groupings via the Games-Howell method to evaluate the varying expression levels of N-terminal detection for the drop-in yeast display reporter with various BY4741 single gene knockout strains via flow cytometry.

			Flow Cytometry Data - Drop-in Yeast Display							
			LeuOmeRS				TyrOmeRS			
			N	Mean	95% CI	Grouping	N	Mean	95% CI	Grouping
No ncAA	N-terminal Detection	BY4741	3	6501	(5316, 7686)	C	3	5021	(4406, 5636)	C
		ΔUPF1	3	16275	(15347, 17202)	A	3	14639	(11834, 17443)	A
		ΔUPF2	3	9628	(9017, 10240)	B	3	7882	(6546, 9218)	B
		ΔUPF3	3	8927	(7715, 10140)	B	3	4955	(-5721, 15630)	A B C D
		ΔTPA1	3	5194	(4067, 6320)	C D	3	4296	(3247, 5346)	C D
		ΔPOP2	3	4701.7	(4324.6, 5078.7)	C D	3	3971	(3432, 4510)	D
		ΔPPQ1	3	4695	(3758, 5632)	D	3	4022	(2811, 5232)	C D
OmeY	N-terminal Detection	BY4741	3	5831	(5030, 6633)	C	3	5582	(5033, 6132)	B C
		ΔUPF1	3	13641	(11791, 15492)	A	3	12060	(10946, 13173)	A
		ΔUPF2	3	7791.7	(7698.6, 7884.7)	B	3	6630	(5276, 7984)	B
		ΔUPF3	3	7565	(5416, 9714)	B C	3	7121	(6067, 8174)	B
		ΔTPA1	3	4564	(3633, 5496)	C	3	4527	(3750, 5303)	C D
		ΔPOP2	3	4008	(3185, 4831)	C	3	4013	(3037, 4989)	D
		ΔPPQ1	3	4268	(3286, 5250)	C	3	4101	(3636, 4567)	D
AzF	N-terminal Detection	BY4741	3	7233.7	(7010.1, 7457.3)	B	3	5567	(4720, 6415)	B C
		ΔUPF1	3	17442	(15792, 19091)	A	3	13832	(9660, 18004)	A
		ΔUPF2	3	8399	(7669, 9130)	B	3	6782	(6296, 7268)	A B
		ΔUPF3	3	8650	(7723, 9576)	B	3	6705	(5958, 7452)	A B
		ΔTPA1	3	4567	(4355.8, 4778.2)	C	3	4090	(3397, 4782)	D
		ΔPOP2	3	5020.3	(4697.0, 5343.7)	C	3	4210	(3588, 4832)	D
		ΔPPQ1	3	5159	(4708, 5610)	C	3	4329	(3481, 5178)	C D

**Means that do not share a letter are statistically different*

Table S13: Primers used for cloning the various reporters.

Primer Name	Primer Sequence	Intended Reaction	DNA Template
N-GFP-F	GTCAAGGAGAAAAAACCCCGGATCGAATTCCCTACTTCATACATTTTCAATTAAGATGTCCAAGGGCGAGGAGCTCTTTAC	Cloning pCTCON2-sfGFP/sfGFP151TAG and pCTCON2-GXB/GYB	pCTCON2-BYG
C-GFP-R	CAGCAGCGGAGCCAGCGGATCCCATCTCGAGCTTATAGAGCTCATCCATGCC	Cloning pCTCON2-GXB/GYB	pCTCON2-BYG
N-BFP-FX	ATGGGATCCGCTGGCTCCGCTGCTGGTTCTGGCGAATAGATGAGCGAGCTGATTAAGGAGAACATG	Cloning pCTCON2-GXB	pCTCON2-BYG
C-BFP-R	GTTACATCTACACTGTTGTTATCAGATCTCGAGCTATTATTAGTGGTGGTGGTGGTGGTGATTAAGCTTGTGCCCCAGTTTGCTAG	Cloning pCTCON2-GXB/GYB	pCTCON2-BYG
N-BFP-FY	ATGGGATCCGCTGGCTCCGCTGCTGGTTCTGGCGAATACATGAGCGAGCTGATTAAGGAGAACATG	Cloning pCTCON2-GYB	pCTCON2-BYG
mTagBFP2-F-pCT	ATCGAGAATTCCCTACTTCATACATTTTCAATTAAGATGAGCGAGCTGATTAAGGAGAAC	Cloning pCTCON2-BXG/BYG	pBAD-mTAGBFP2
mTagBFP2-R-pCT	ATCGAGGATCCCATATTAAGCTTGTGCCCCAGTTTGC	Cloning pCTCON2-BXG/BYG	pBAD-mTAGBFP2
GFP-151F	CTGGAGTATAATTTCAATTCCCATAATGTATAGATTACCGCAGATAAGCAAAAGAATGGC	Cloning pCTCON2-sfGFP151TAG	pCTCON2-BYG
GFP-151R	GCCATTCTTTTGCTTATCTGCGGTAATCTATACATTATGGGAATTGAAATTATACTCCAG	Cloning pCTCON2-sfGFP151TAG	pCTCON2-BYG
Rev-BglII-HIS	GTTACATCTACACTGTTGTTATCAGATCTCGAGCTATTATTAGTGGTGGTGGTGGTGGTG	Cloning pCTCON2-sfGFP151TAG and pCTCON2-sfGFP	pCTCON2-BYG
pCTCON2-BFP-Fwd	TTAACGTCAAGGAGAAAAAACCCCGGATCG	Amplify BFP-GFP from pCTCON2 construct	pCTCON2-BXG
pCTCON2-GFP-Rev	GAGCTCATCCATGCCATGAGTAATGCCTGC	Amplify BFP-GFP from pCTCON2 construct	pCTCON2-BXG
RCFwd_1TAG_BFPGFP	GCCCTTGGATGCGTATTCGCCAGAACCAGCAGCGGAGCCAGCCTATCCCATATTAAGCTT	Amplify BFP segment with altTAG location	pCTCON2-BXG
Fwd_1TAG_BFPGFP	AAGCTTAATATGGGATAGGCTGGCTCCGCTGCTGGTTCTGGCGAATACGCATCCAAGGGC	Amplify GFP segment with altTAG location	pCTCON2-BXG
RCForward_AltTAG2_BFPGFP	GCCCTTGGATGCGTATTCGCCAGAACCAGCAGCCTAGCCAGCGGATCCCATATTAAGCTT	Amplify BFP segment with altTAG2 location	pCTCON2-BYG
Forward_AltTAG2_BFPGFP	AAGCTTAATATGGGATCCGCTGGCTAGGCTGCTGGTTCTGGCGAATACGCATCCAAGGGC	Amplify GFP segment with altTAG2 location	pCTCON2-BYG
RCForward_AltTAG3_BFPGFP	GCCCTTGGATGCGTATTCGCCAGAACCCTAAGCGGAGCCAGCGGATCCCATATTAAGCTT	Amplify BFP segment with altTAG3 location	pCTCON2-BYG
Forward_AltTAG3_BFPGFP	AAGCTTAATATGGGATCCGCTGGCTCCGCTTAGGGTTCTGGCGAATACGCATCCAAGGGC	Amplify GFP segment with altTAG3 location	pCTCON2-BYG
RCForward_AltTAG4_BFPGFP	GCCCTTGGATGCGTATTCGCCCTAACCAGCAGCGGAGCCAGCGGATCCCATATTAAGCTT	Amplify BFP segment with altTAG4 location	pCTCON2-BYG

Forward_AltTAG4_BFPGFP	AAGCTTAATATGGGATCCGCTGGCTCCGCTGCTGGTTAGGGCGAATACGCATCCAAGGGC	Amplify GFP segment with altTAG4 location	pCTCON2-BYG
RCFwd_2TAG_BFPGFP	GCCCTTGGATGCCTATTCGCCAGAACCAGCAGCGGAGCCAGCCTATCCCATATTAAGCTT	Amplify BFP segment with 2TAG location	pCTCON2-BXG
Fwd_2TAG_BFPGFP	AAGCTTAATATGGGATAGGCTGGCTCCGCTGCTGGTTCTGGCGAATAGGCATCCAAGGGC	Amplify GFP segment with 2TAG location	pCTCON2-BXG
pCTCON2-XbaI-fwd-Gibson	AGCTGGAGCTCCACCGCGGTGGCGGCCGCTCTAGAGCTGGTACCAATTCCTTGAATTTTC	Amplify reporter from pCTCON2 vector to pRS416 vector	pCTCON2-BXG-altTAG, pCTCON2-BXG
Gibson SalI Rev	GCGAATTGGGTACCGGGCCCCCCCTCGAGGTCGACCGAATTGGAGCTCAATTCTCTTAGG	Amplify reporter from pCTCON2 vector to pRS416 vector	pCTCON2-BXG-altTAG, pCTCON2-BXG
L1TAGfwd	GCGGTAGCGGAGGCGGAGGGTCGGCTAGCTAGATACAGATGACTCAAAGTCCCAGTTCACTA	Used to introduce a TAG codon on the L1 position	pRS416-Aga1p-FAPB2.3.6
L1TAGrev	TAGTGAACTGGGACTTTGAGTCATCTGTATCTAGCTAGCCGACCCTCCGCCTCCGCTACCGC	Used to introduce a TAG codon on the L1 position	pRS416-Aga1p-FAPB2.3.6
Aga1p-G2957A-FWD	ACCATTGATGAAGTTTGGTATTGTATGGAGATTGAAGTAGTGGAAACTTCTGTAGTGGT	Used to fix mutation in Aga1p for the WT constructs	pRS416-Aga1p-FAPB2.3.6
Aga1p-G2957A-REV	TACCACTACAGAAGTTTCCACTACTTCAATCTCCATACAATACCAAACTTCATCAATGGT	Used to fix mutation in Aga1p for the WT constructs	pRS416-Aga1p-FAPB2.3.6
1-DROPIN-Rv3	AACCCTCACTAAAGGGAACAAAAGCTGGGTACCTTAACTGAAAATTACATTGCAAGCAAC	Used to amplify Aga1p from YIP sHRPa-Aga1p	YIP sHRPa-Aga1p
2-DROPIN-Fv3	AATATTGCCTTGGCATCTGATCCAGAAACGATTCTAGTGACGATAACCAAGACAAACGAT	Used to amplify Aga1p from YIP sHRPa-Aga1p	YIP sHRPa-Aga1p
3-DROPIN-Rv3	ATCGTTTGTCTTGGTTATCGTCACTAGAATCGTTTCTGGATCAGATGCCAAGGCAATATT	Used to amplify the region between GAL1-10 and Aga1p overlap in pCTCON2	pCTCON2
4-DROPIN-Fv3	AAAGTAAGAATTTTTGAAAATTCAATATAAATGACATTATCTTTCGCTCATTTTACCTAC	Used to amplify the region between GAL1-10 and Aga1p overlap in pCTCON2	pCTCON2
pRS416Aga1pXbaIJSFwd	GCTGGAGCTCCACCGCGGTGGCGGCCGCTCTAGAGGTACCTTAACTGAAAATTACATTGC	Updated primer from KpnI forward for Aga1p cloning in pRS416	pCTCON2-Aga1p-FAPB2.3.6
Con2seqfwd	GTTCCAGACTACGCTCTGCAG	Used to amplify FAPB2.3.6 and FAPB2.3.6L1TAG for cloning into pCTCON2-Aga1p	pCTCON2-FAPB2.3.6 and pCTCON2-FAPB2.3.6L1TAG
Con2seqrev	GATTTTGTTACATCTACACTGTT	Used to amplify FAPB2.3.6 and FAPB2.3.6L1TAG for cloning into pCTCON2-Aga1p	pCTCON2-FAPB2.3.6 and pCTCON2-FAPB2.3.6L1TAG

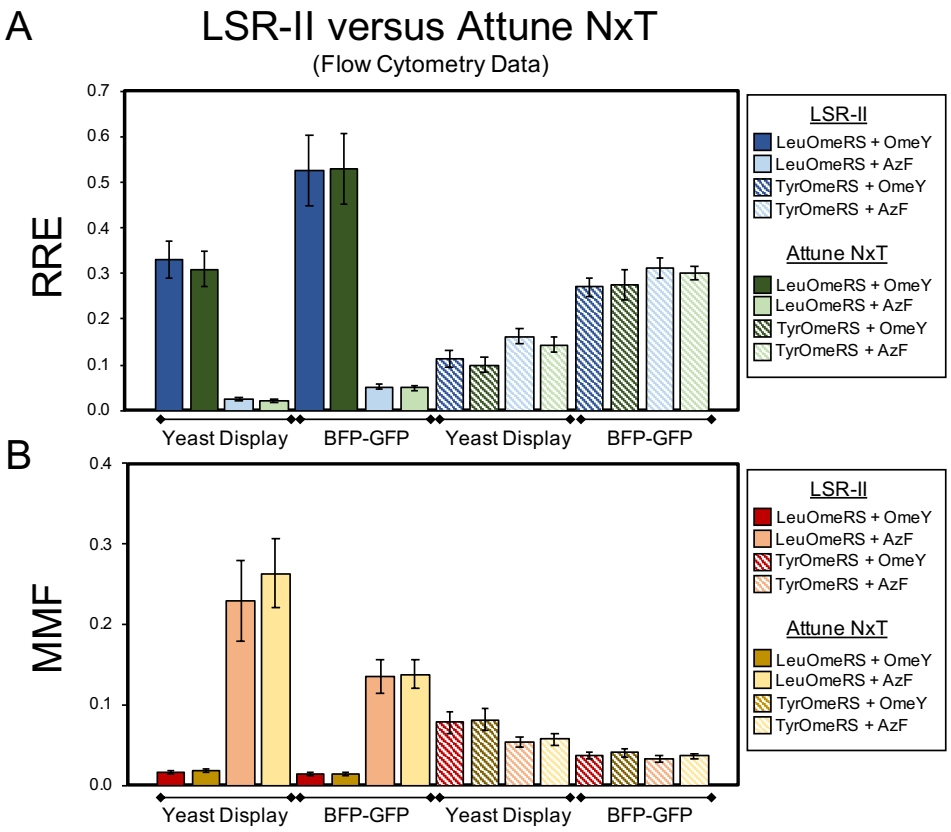

Fig. S1: Comparison of measurements of ncAA incorporation between two different flow cytometers (LSR-II and Attune NxT). Yeast display and BFP-GFP fluorescent reporter calculations of (A) relative readthrough efficiency (RRE) and (B) maximum misincorporation frequency (MMF) with four orthogonal translation system-ncAA combinations run on both the LSR-II and Attune NxT. Cells from the same induced cultures were run on each instrument in these experiments. For a summary of statistical analyses comparing the datasets obtained on the different instruments, see Table S13.

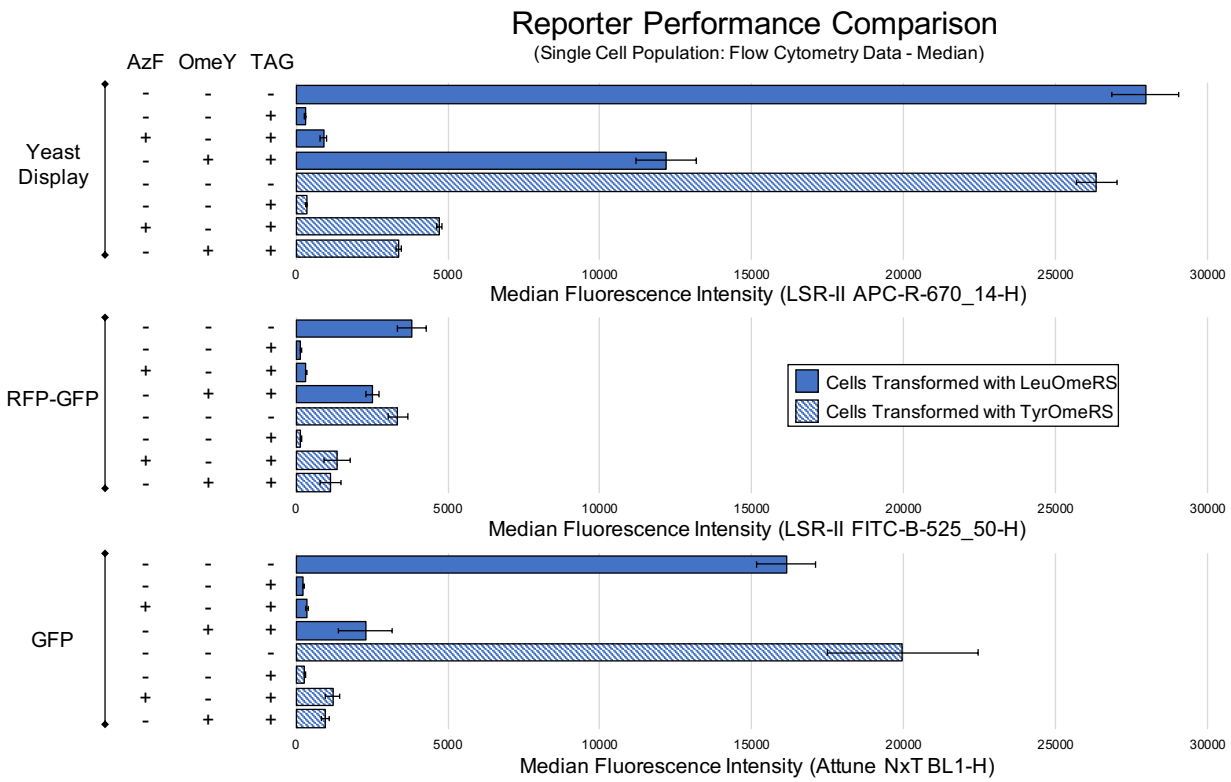

Fig. S2: Reporter performance comparison. Quantification of ncAA incorporation efficiency for four orthogonal translation system-ncAA combinations performed with yeast display, a RFP-GFP dual-fluorescent protein reporter, and a sfGFP single-fluorescent protein reporter. Performance was evaluated with an alternative analysis method using the median fluorescence intensity of the gated single cell population (see Materials and Methods for details). The condition denoted by absence of ncAAs and a TAG codon is the wild-type reporter construct induced in the absence of ncAAs.

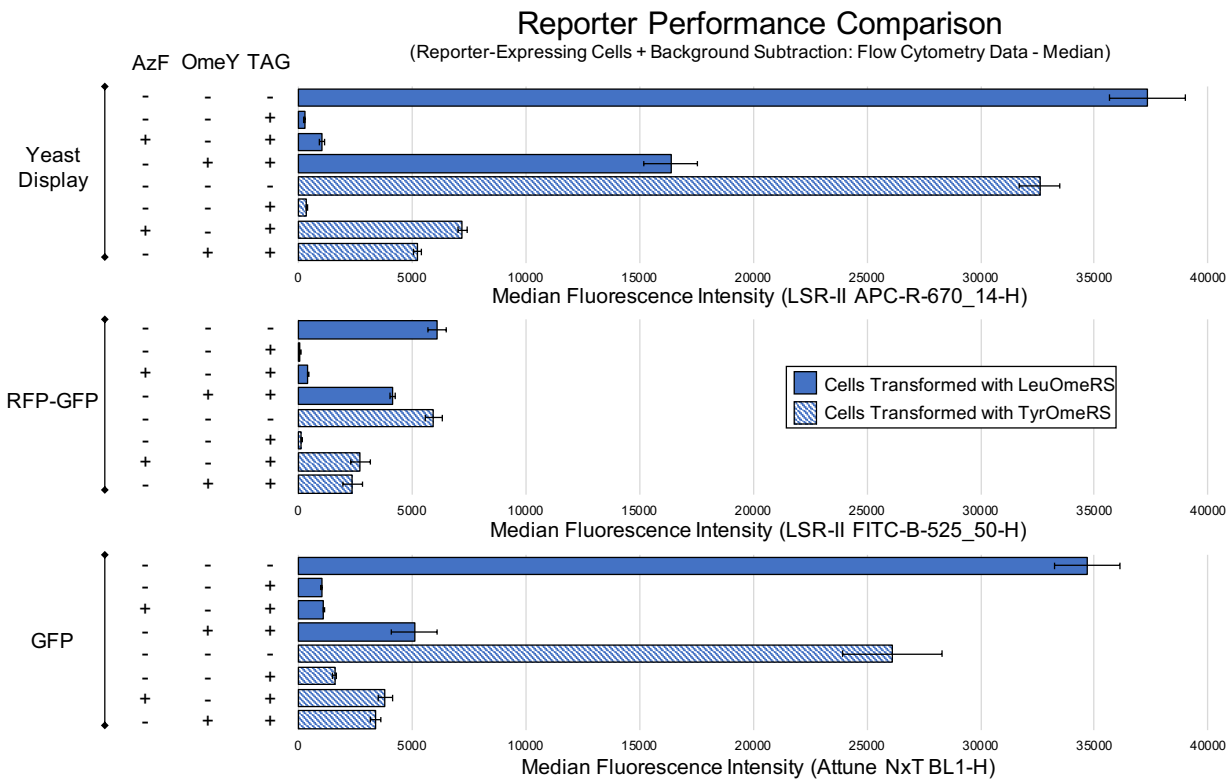

Fig. S3: Reporter performance comparison. Quantification of ncAA incorporation efficiency for four orthogonal translation system-ncAA combinations performed with yeast display, a RFP-GFP dual-fluorescent protein reporter, and a sfGFP single-fluorescent protein reporter. Performance was evaluated with an alternative analysis method using the median fluorescence intensity of reporter-expressing cells with background subtraction. The condition denoted by absence of ncAAs and a TAG codon is the wild-type reporter construct induced in the absence of ncAAs.

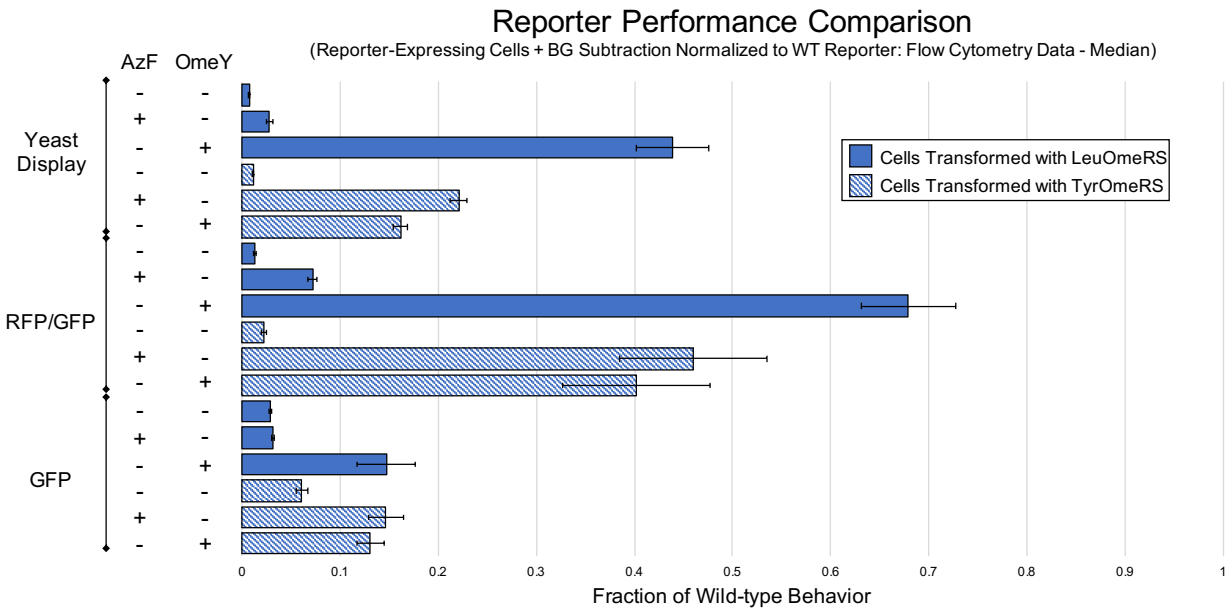

Fig. S4: Reporter performance comparison. Quantification of ncAA incorporation efficiency for four orthogonal translation system-ncAA combinations performed with yeast display, a RFP-GFP dual-fluorescent protein reporter, and a sfGFP single-fluorescent protein reporter. Performance was evaluated with an alternative analysis method using the median fluorescence intensity of reporter-expressing cells with background subtraction and normalization to the median fluorescence intensity of the cells expressing the wild-type construct induced in the absence of ncAAs (see Materials and Methods for details).

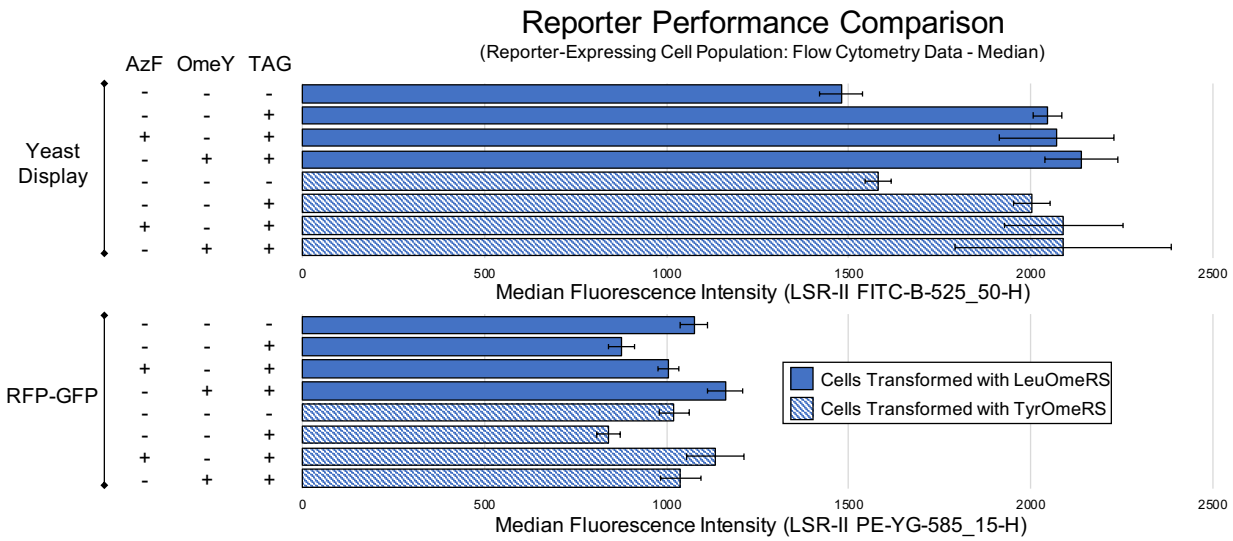

Fig. S5: Reporter performance comparison. Measurement of reporter expression level (either yeast display or a RFP-GFP dual-fluorescent protein reporter) with an alternative analysis method using the median fluorescence intensity of the cell population exhibiting above-background reporter expression. The condition denoted by absence of ncAAs and a TAG codon is the wild-type reporter construct induced in the absence of ncAAs.

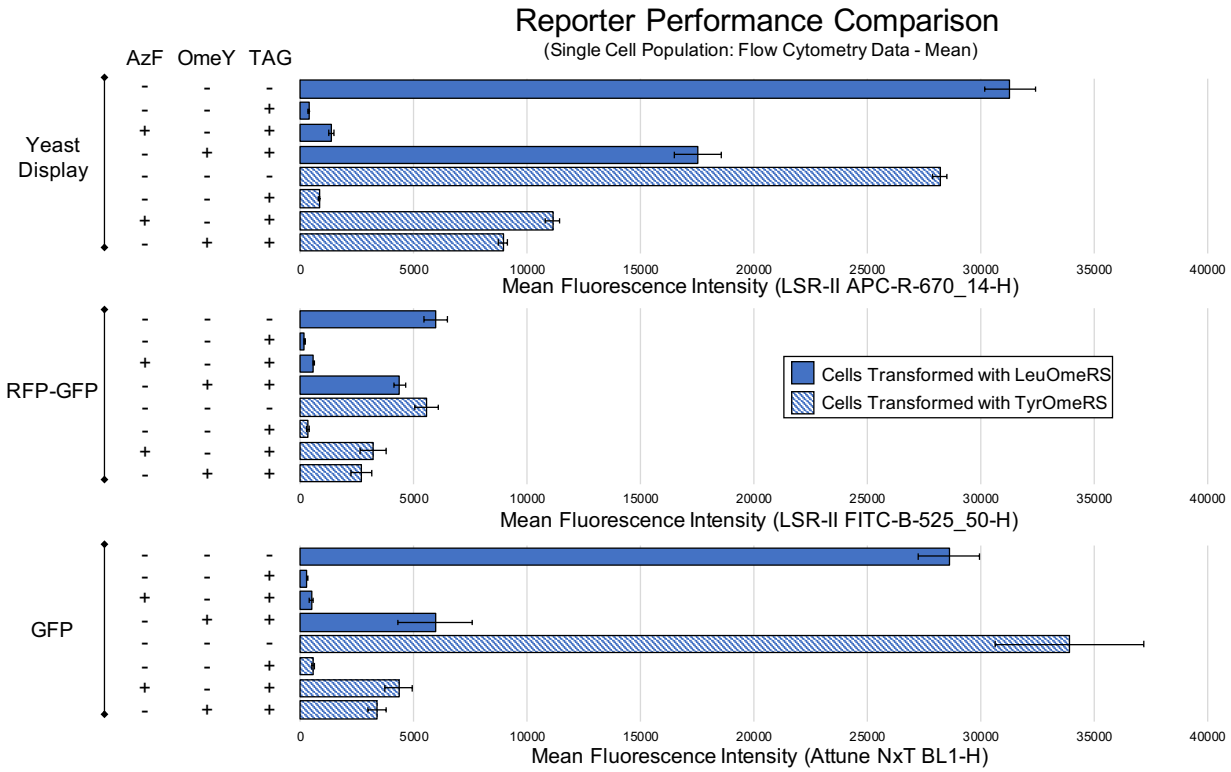

Fig. S6: Reporter performance comparison. Quantification of ncAA incorporation efficiency for four orthogonal translation system-ncAA combinations performed with yeast display, a RFP-GFP dual-fluorescent protein reporter, and a sfGFP single-fluorescent protein reporter. Performance was evaluated with an alternative analysis method using the mean fluorescence intensity of the single cell population. The condition denoted by absence of ncAAs and a TAG codon is the wild-type reporter construct induced in the absence of ncAAs.

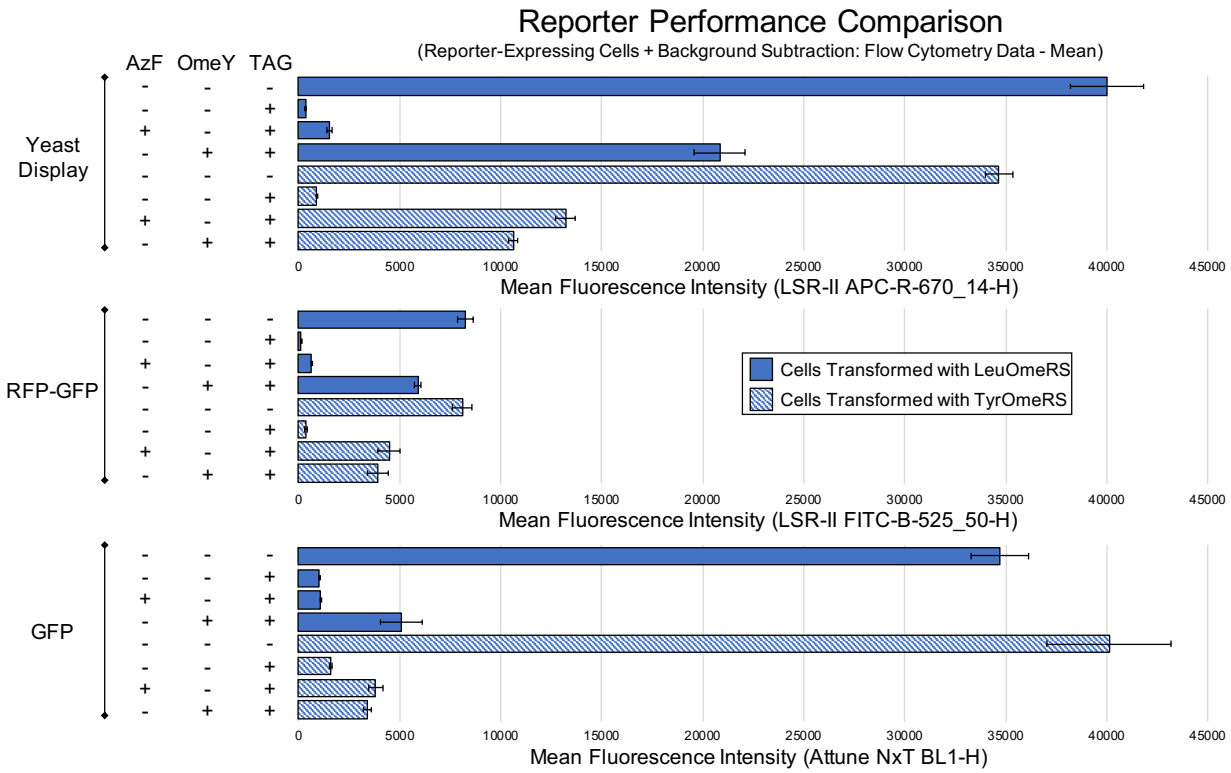

Fig. S7: Reporter performance comparison. Quantification of ncAA incorporation efficiency for four orthogonal translation system-ncAA combinations performed with yeast display, a RFP-GFP dual-fluorescent protein reporter, and a sfGFP single-fluorescent protein reporter. Performance was evaluated with an alternative analysis method using the mean fluorescence intensity of reporter-expressing cells with background subtraction. The condition denoted by absence of ncAAs and a TAG codon is the wild-type reporter construct induced in the absence of ncAAs.

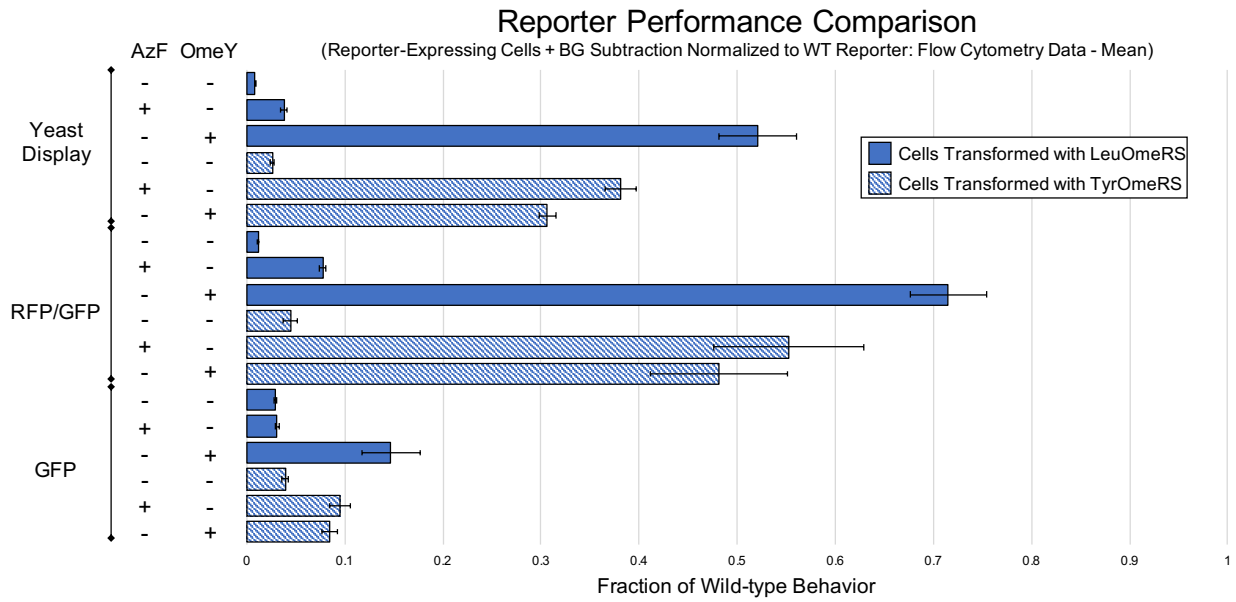

Fig. S8: Reporter performance comparison. Quantification of ncAA incorporation efficiency for four orthogonal translation system-ncAA combinations performed with yeast display, a RFP-GFP dual-fluorescent protein reporter, and a sfGFP single-fluorescent protein reporter. Performance was evaluated with an alternative analysis method using the mean fluorescence intensity of reporter-expressing cells with background subtraction and normalized to the mean fluorescence intensity of the cells expressing the wild-type construct induced in the absence of ncAAs.

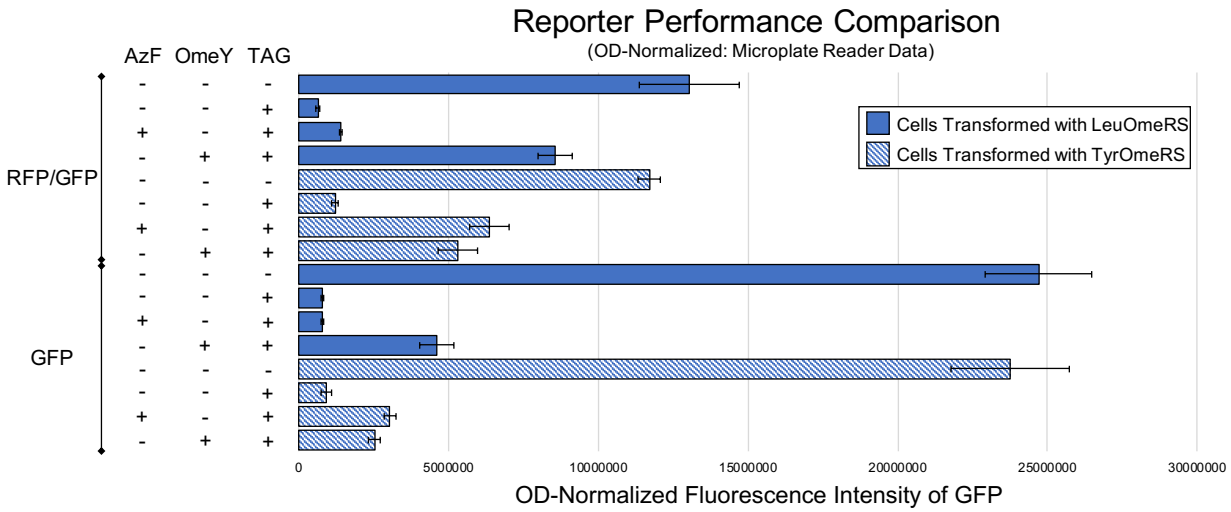

Fig. S9: Reporter performance comparison. Quantification of ncAA incorporation efficiency for four orthogonal translation system-ncAA combinations performed with a RFP-GFP dual-fluorescent protein reporter, and a sfGFP single-fluorescent protein reporter and analyzed on a microplate reader. Performance was evaluated with an alternative analysis method using sample fluorescence normalized to sample OD600. The condition denoted by absence of ncAAs and a TAG codon is the wild-type reporter construct induced in the absence of ncAAs.

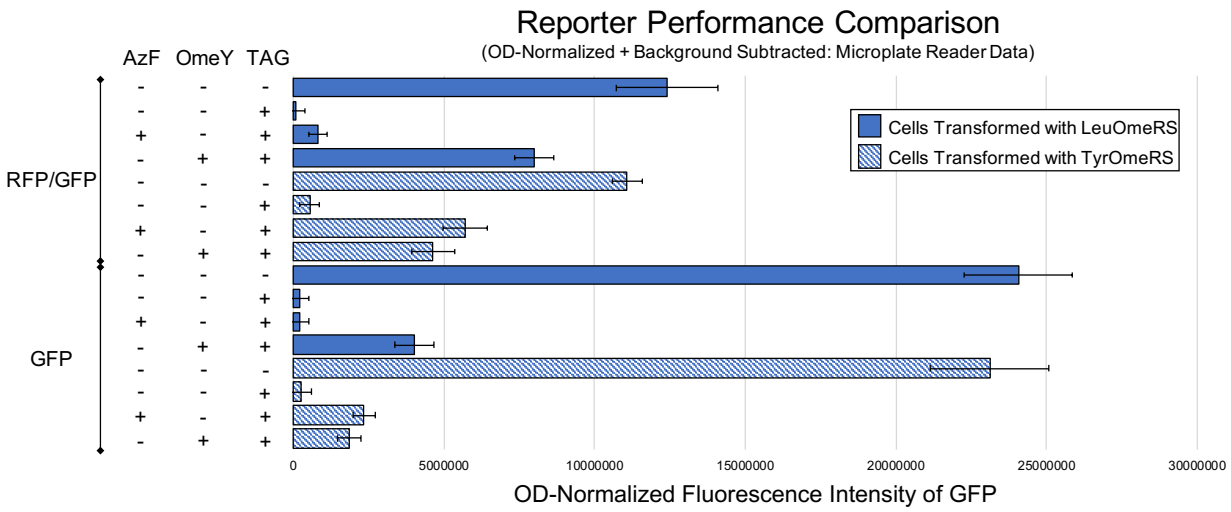

Fig. S10: Reporter performance comparison. Quantification of ncAA incorporation efficiency for four orthogonal translation system-ncAA combinations performed with a RFP-GFP dual-fluorescent protein reporter, and a sfGFP single-fluorescent protein reporter and analyzed on a microplate reader. Performance was evaluated with an alternative analysis method using sample fluorescence normalized to sample OD600 and followed by background subtraction to account for cellular autofluorescence. The condition denoted by absence of ncAAs and a TAG codon is the wild-type reporter construct induced in the absence of ncAAs.

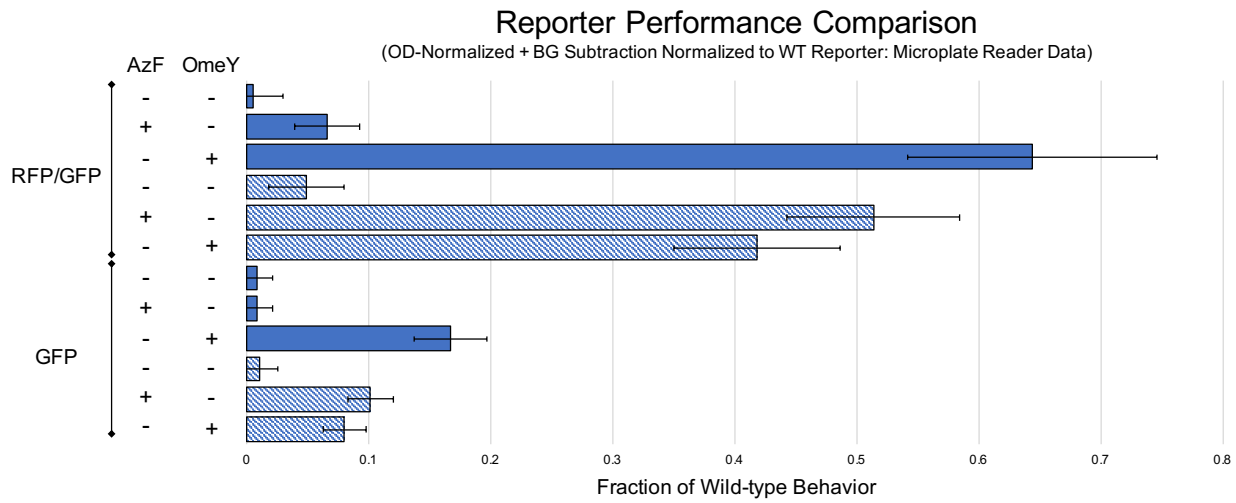

Fig. S11: Reporter performance comparison. Quantification of ncAA incorporation efficiency for four orthogonal translation system-ncAA combinations performed with a RFP-GFP dual-fluorescent reporter, and a sfGFP single-fluorescent reporter. Performance was evaluated with an alternative analysis method using sample fluorescence normalized to sample OD600 with background subtraction and normalization to the cells expressing the wild-type reporter (also OD600 normalized) induced in the absence of ncAAs.

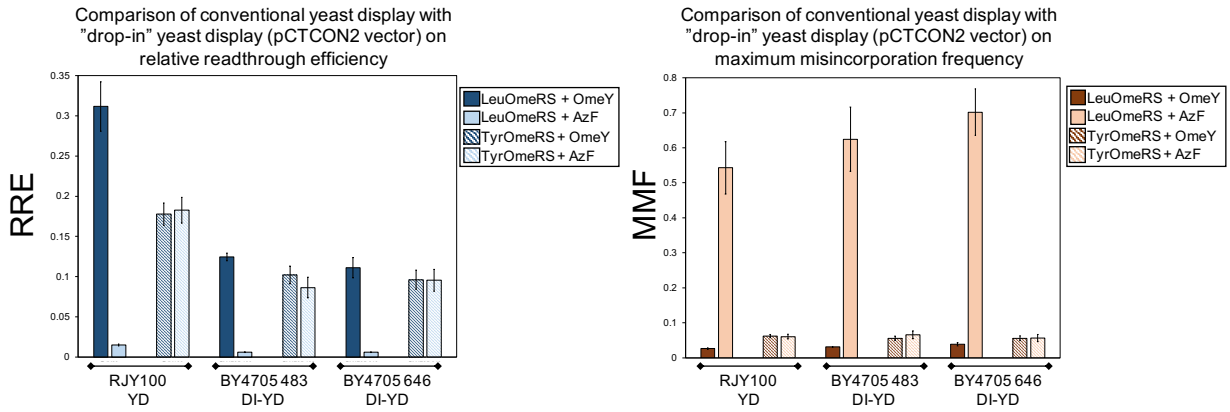

Figure S12: Conventional yeast display (YD) versus drop-in yeast display (DI-YD). Quantification of ncAA incorporation efficiency and fidelity for conventional display (in RJY100) and drop-in display (in multiple ΔTRP1 strains) in a pCTCON2 vector.

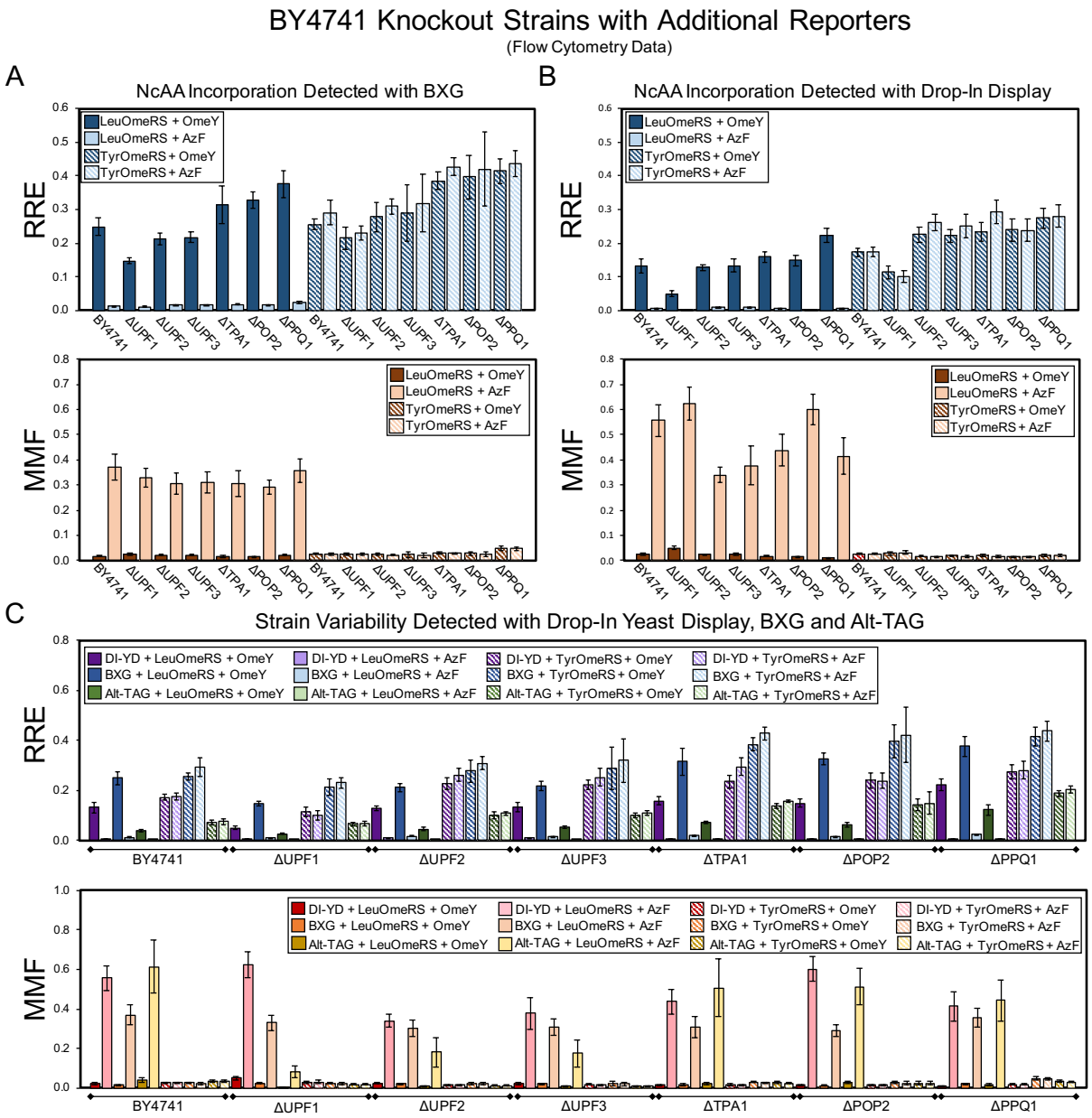

Figure S13: Evaluation of ncAA incorporation events in a series of single-gene knockout strains using two dual-fluorescent protein reporters and a drop-in yeast display (DI-YD) reporter. (A) Measurements of ncAA incorporation efficiency and fidelity in BY4741 and six single-gene knockouts of BY4741 using the BXG BFP-GFP reporter in a pRS416 (URA3 marker) plasmid backbone. (B) Measurements of ncAA incorporation efficiency and fidelity in BY4741 and six single-gene knockouts of BY4741 using the drop-in yeast display reporter in a pRS416 (URA3 marker) plasmid backbone. (C) Complete set of ncAA incorporation measurements for efficiency and fidelity using the Alt-TAG BFP-GFP reporter, BXG BFP-GFP reporter, and drop-in yeast display reporter in pRS416 (URA marker) plasmid backbones. All conditions reported here were evaluated with end point measurements in biological triplicate. The statistical analyses for these data can be found in Tables S7-S12.

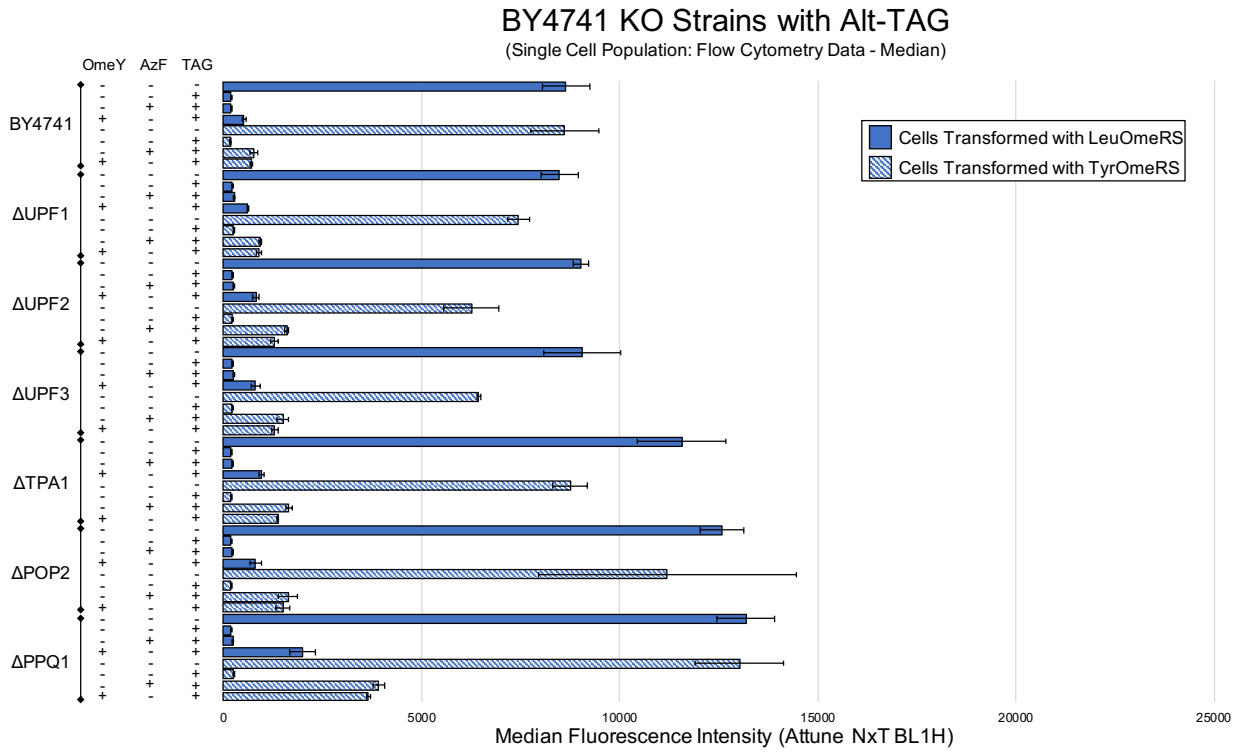

Fig. S14: Alternate analysis of BY4741 and six single-gene knockout strains using the Alt-TAG BFP-GFP dual-fluorescent protein reporter. Measurements for the efficiency of ncAA incorporation calculated with median fluorescence intensity using single cell population analysis as described in Materials and Methods Section 2.11. The condition denoted by absence of ncAAs and a TAG codon is the wild-type reporter construct induced in the absence of ncAAs.

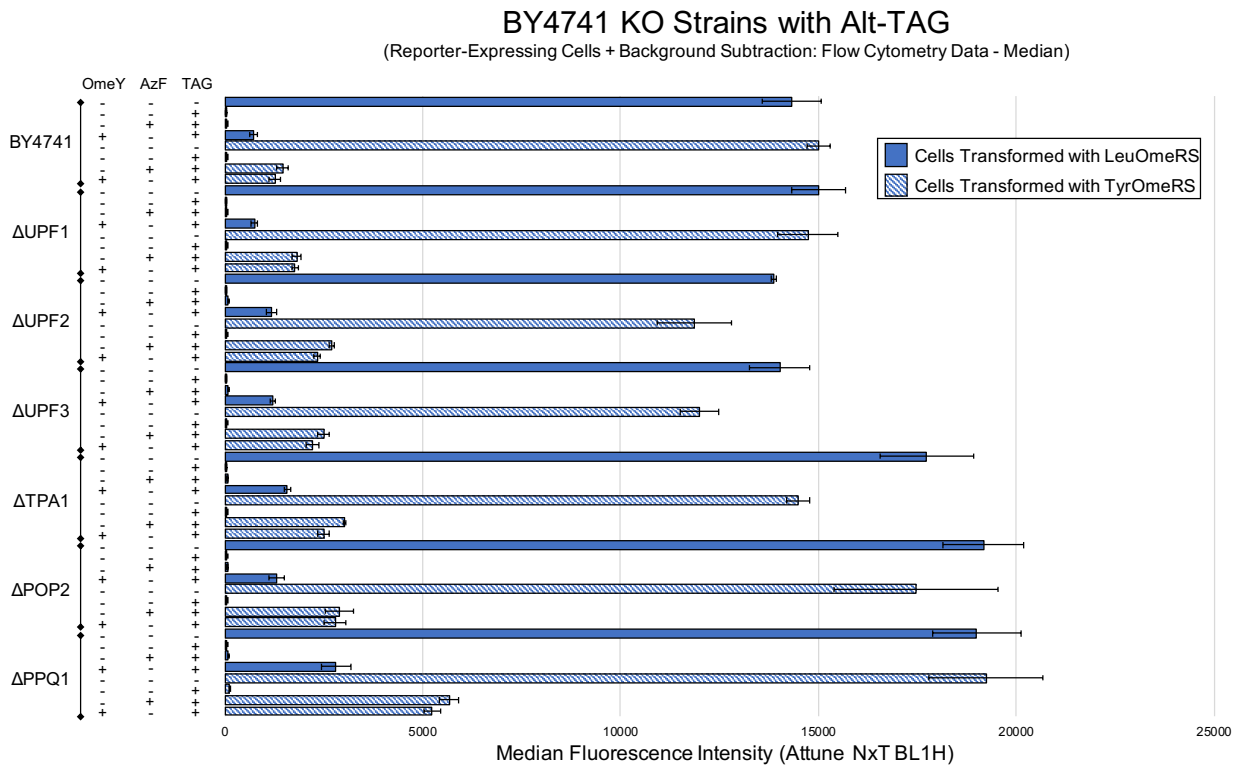

Fig. S15: Alternate analysis of BY4741 and six single-gene knockout strains using the Alt-TAG BFP-GFP dual-fluorescent protein reporter. Measurements for the efficiency of ncAA incorporation calculated using the median fluorescence intensity of reporter-expressing cells with background subtraction as described in Materials and Methods Section 2.11. The condition denoted by absence of ncAA and TAG codon is the wild-type reporter construct induced in the absence of ncAAs.

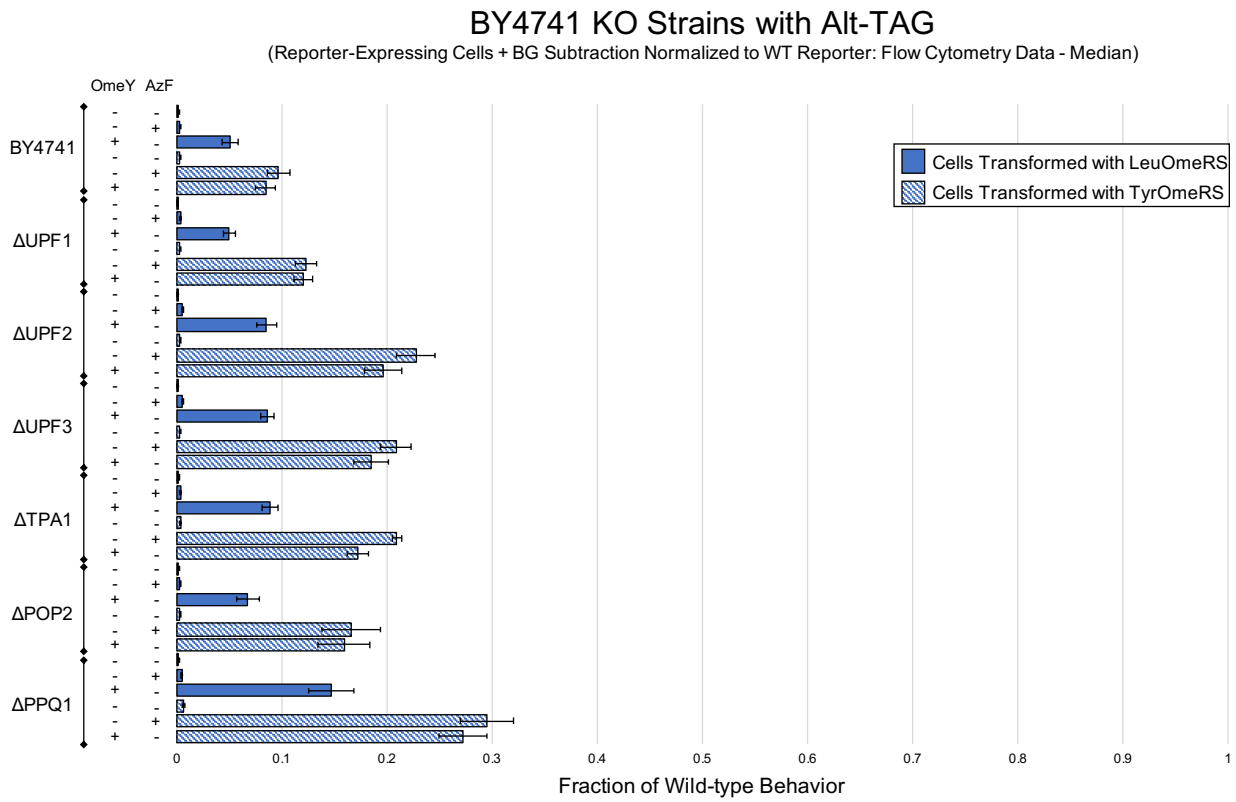

Fig. S16: Alternate analysis of BY4741 and six single-gene knockout strains using the Alt-TAG BFP-GFP dual-fluorescent protein reporter. Measurements for the efficiency of ncAA incorporation calculated using the median fluorescence intensity of reporter-expressing cells with background subtraction and normalized to expression levels of cells expressing the wild-type reporter induced in the absence of ncAAs.

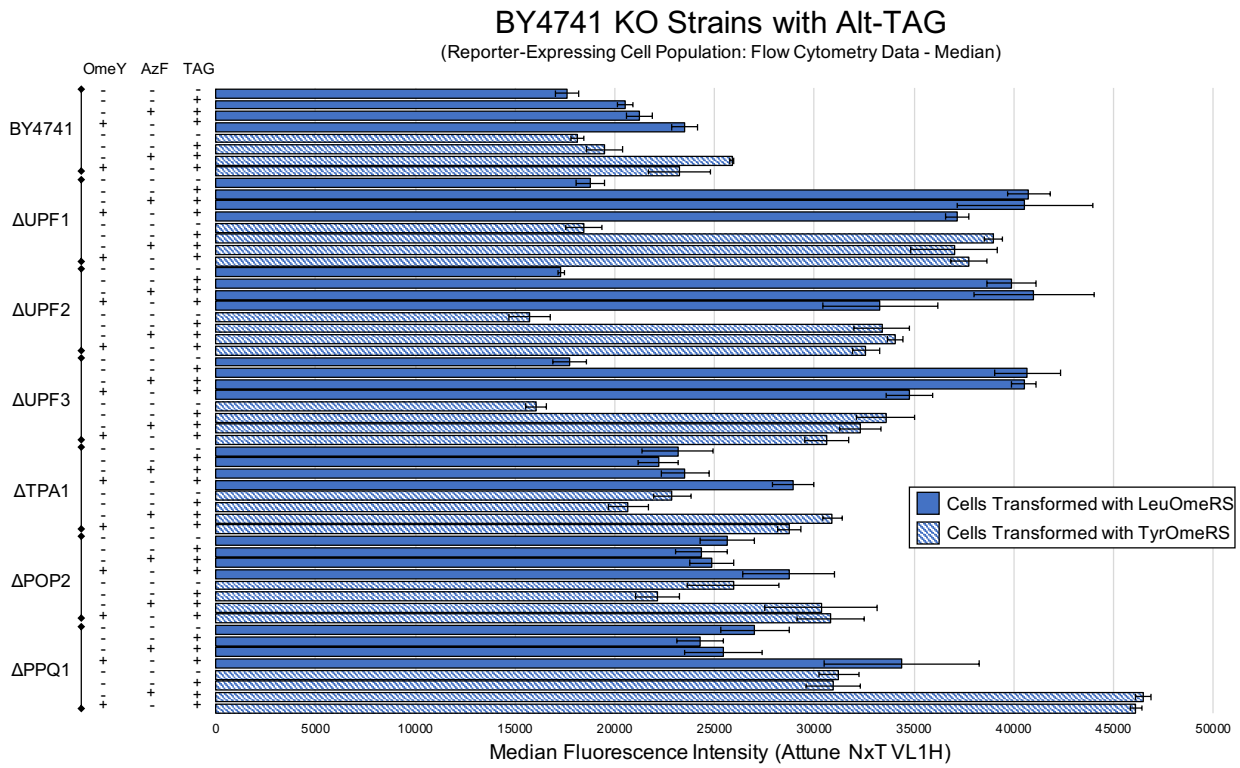

Fig. S17: Measurement of reporter expression level in BY4741 and six single-gene knockout strains containing Alt-TAG BFP-GFP using the median fluorescence intensity of the cell population exhibiting above-background reporter expression. The condition denoted by absence of ncAAs and a TAG codon is the wild-type reporter construct induced in the absence of ncAAs.

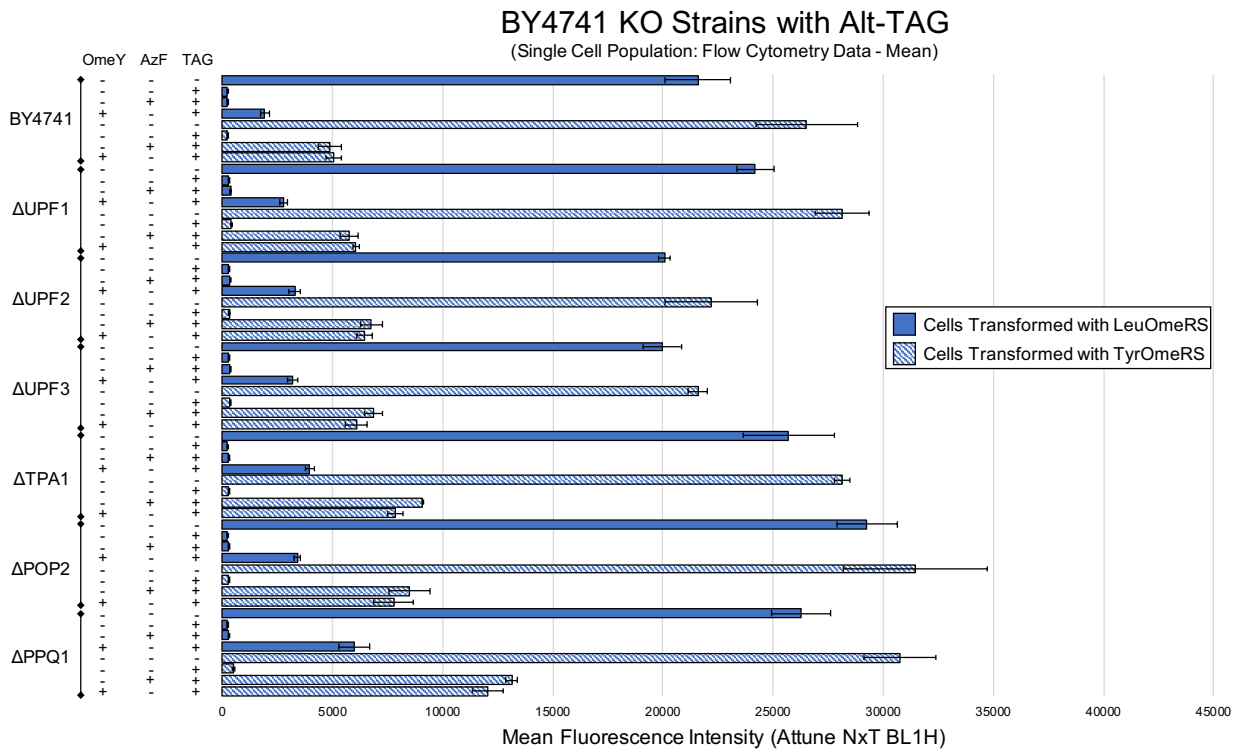

Fig. S18: Alternate analysis of BY4741 and six single-gene knockout strains using the Alt-TAG BFP-GFP dual-fluorescent protein reporter. Performance was evaluated using the mean fluorescence intensity of the single cell population. The condition denoted by absence of ncAAs and a TAG codon is the wild-type reporter construct induced in the absence of ncAAs.

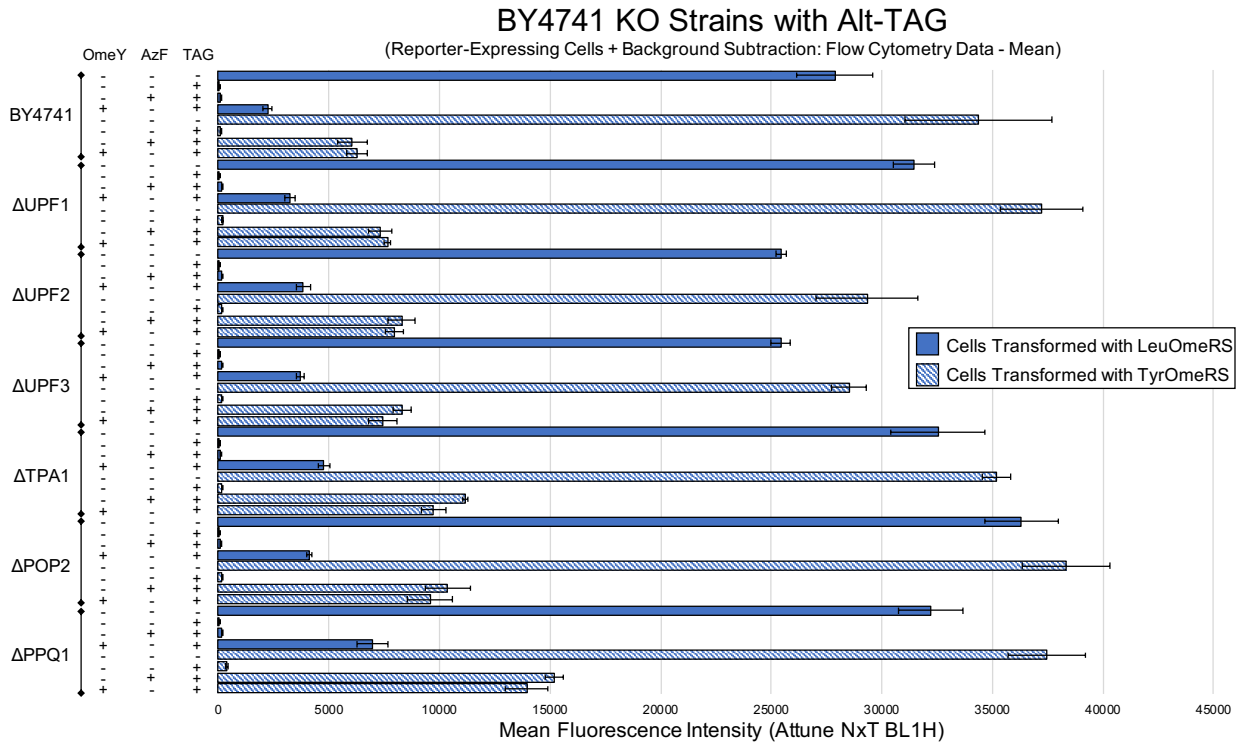

Fig. S19: Alternate analysis of BY4741 and six single-gene knockout strains using the Alt-TAG BFP-GFP dual-fluorescent protein reporter. Performance was evaluated using the mean fluorescence intensity of reporter-expressing cells with background subtraction. The condition denoted by absence of ncAAs and a TAG codon is the wild-type reporter construct induced in the absence of ncAAs.

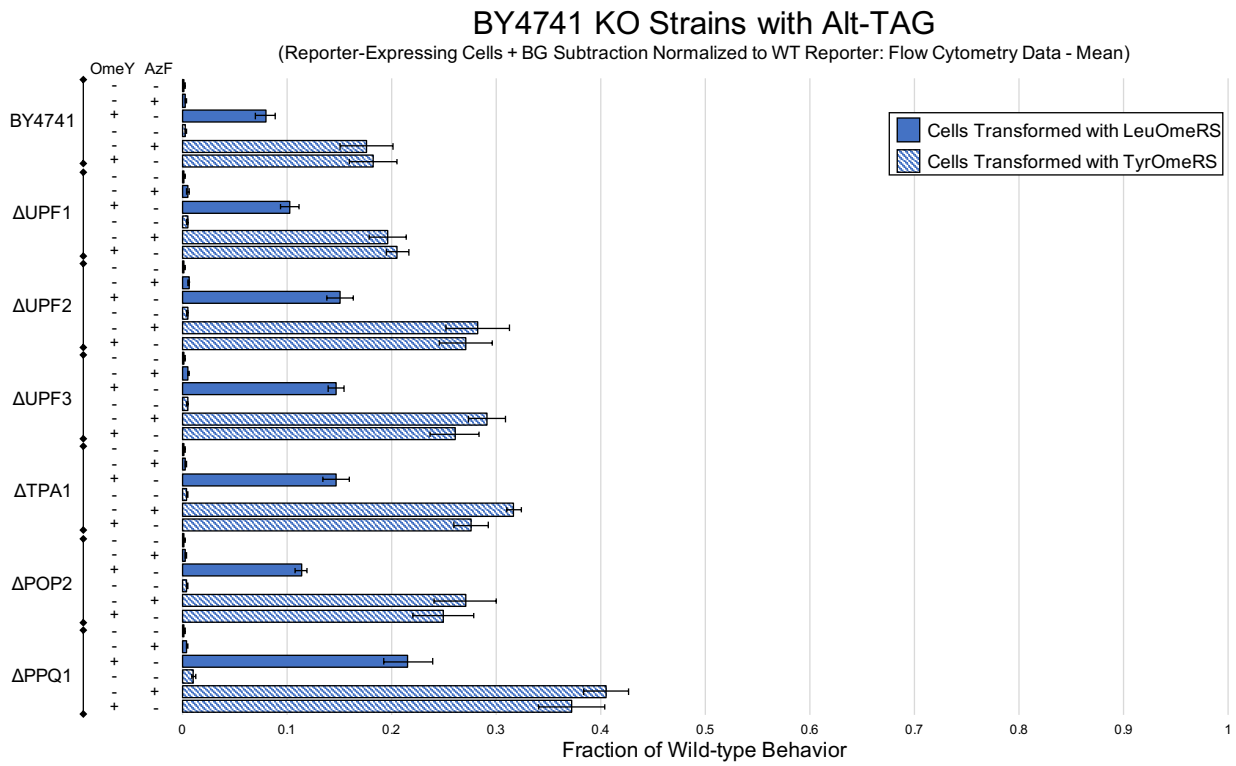

Fig. S20: Alternate analysis of BY4741 and six single-gene knockout strains using the Alt-TAG BFP-GFP dual-fluorescent protein reporter. Measurements for the efficiency of ncAA incorporation calculated using the mean fluorescence intensity of reporter-expressing cells with background subtraction and normalized to mean expression levels of cells expressing the wild-type reporter induced in the absence of ncAAs.

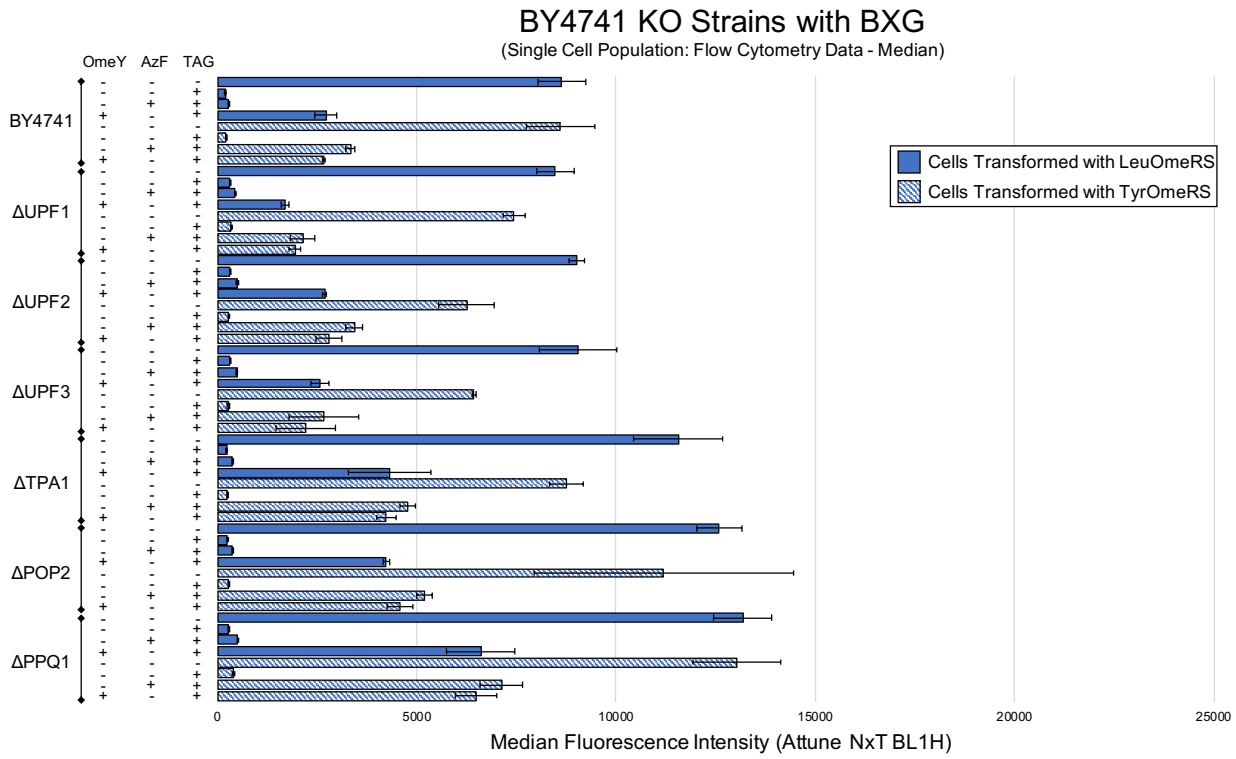

Fig. S21: Alternate analysis of BY4741 and six single-gene knockout strains using the BXG BFP-GFP dual-fluorescent protein reporter. Measurements for the efficiency of ncAA incorporation calculated with median fluorescence intensity using single cell population analysis as described in Materials and Methods Section 2.11. The condition denoted by absence of ncAAs and a TAG codon is the wild-type reporter construct induced in the absence of ncAAs.

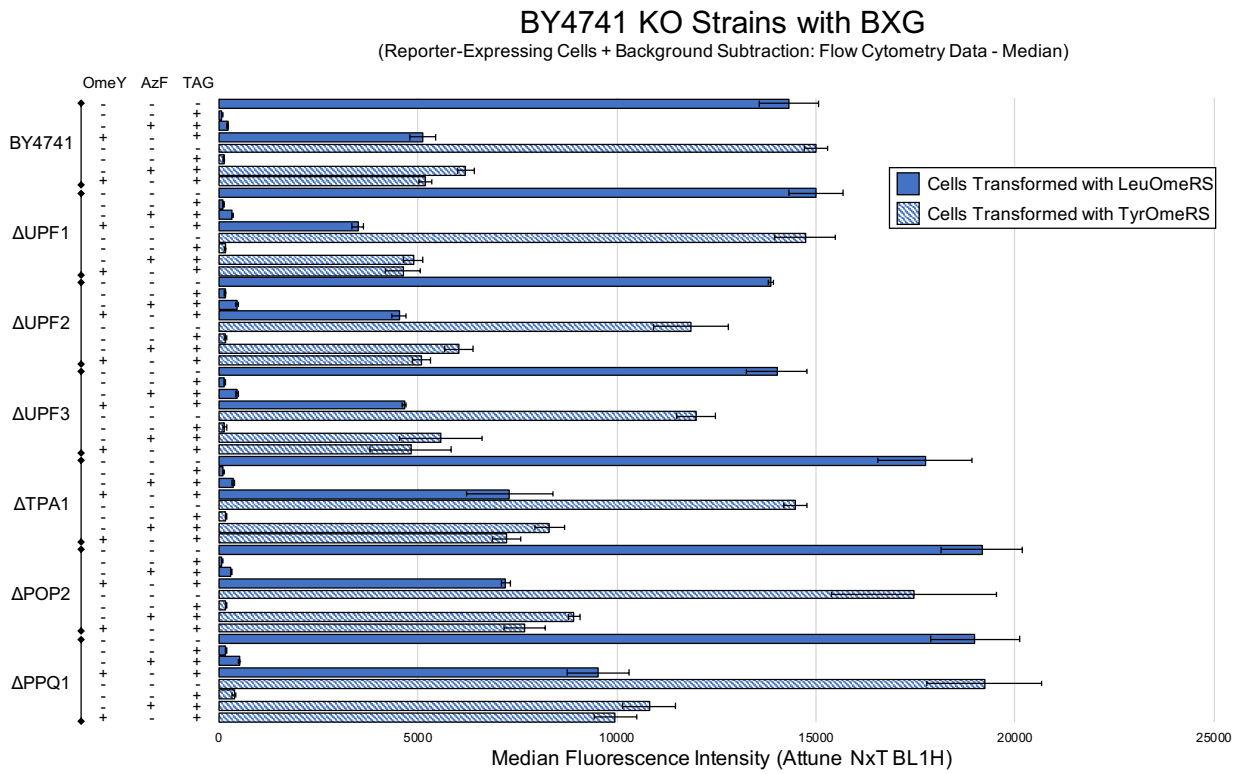

Fig. S22: Alternate analysis of BY4741 and six single-gene knockout strains using the BXG BFP-GFP dual-fluorescent protein reporter. Measurements for the efficiency of ncAA incorporation calculated with median fluorescence intensity using reporter-expressing cells with background subtraction. The condition denoted by absence of ncAAs and a TAG codon is the wild-type reporter construct induced in the absence of ncAAs.

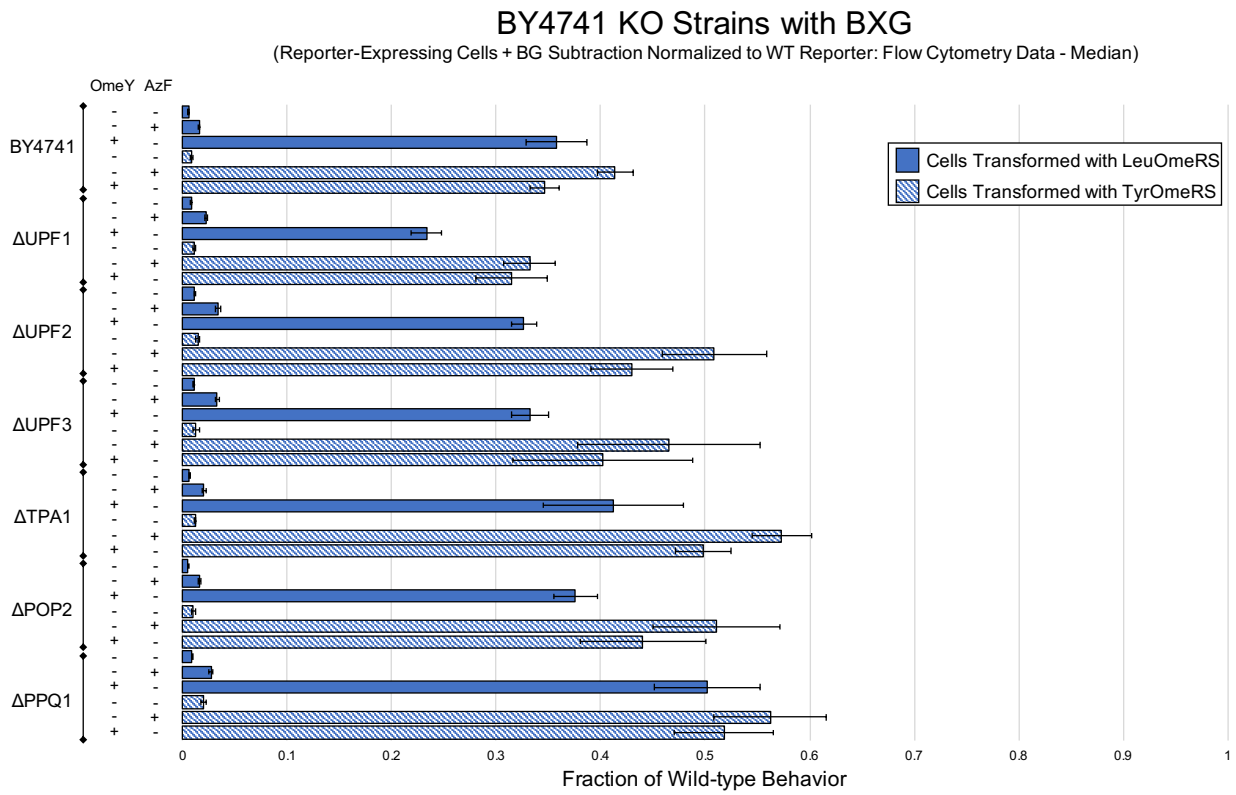

Fig. S23: Alternate analysis of BY4741 and six single-gene knockout strains using the BXG BFP-GFP dual-fluorescent protein reporter. Measurements for the efficiency of ncAA incorporation calculated using the median fluorescence intensity of reporter-expressing cells with background subtraction and normalized to expression levels of cells expressing the wild-type reporter induced in the absence of ncAAs.

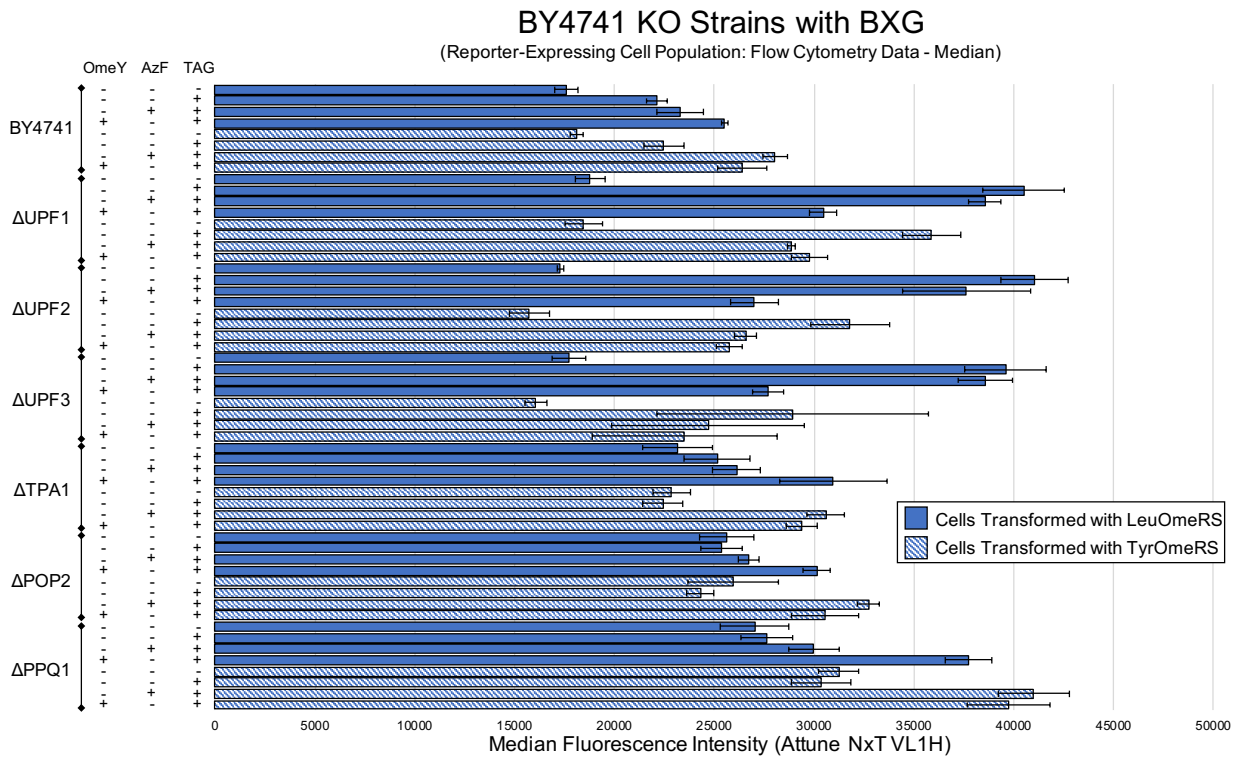

Fig. S24: Measurement of reporter expression level in BY4741 and six single-gene knockout strains containing BXG BFP-GFP using the median fluorescence intensity of the cell population exhibiting above-background reporter expression. The condition denoted by absence of ncAAs and a TAG codon is the wild-type reporter construct induced in the absence of ncAAs.

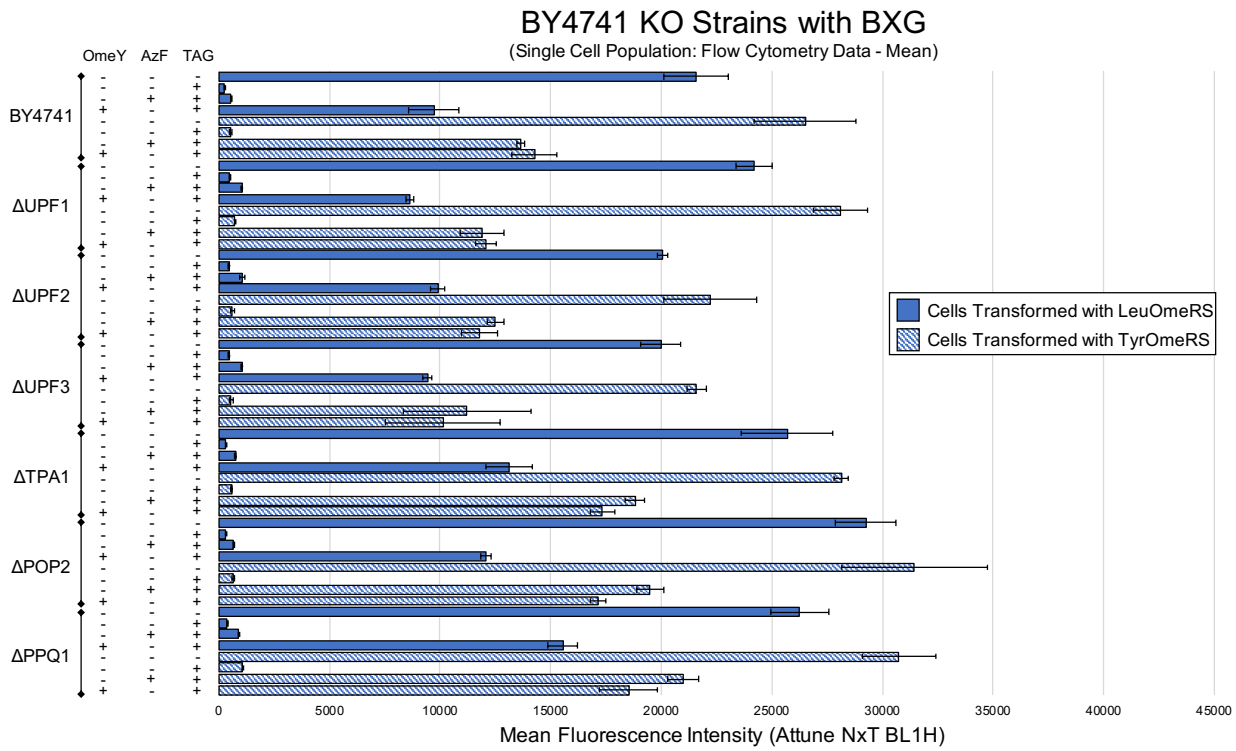

Fig. S25: Alternate analysis of BY4741 and six single-gene knockout strains using the BXG BFP-GFP dual-fluorescent protein reporter. Measurements for the efficiency of ncAA incorporation calculated with mean fluorescence intensity using single cell population analysis as described in Materials and Methods Section 2.11. The condition denoted by absence of ncAAs and a TAG codon is the wild-type reporter construct induced in the absence of ncAAs.

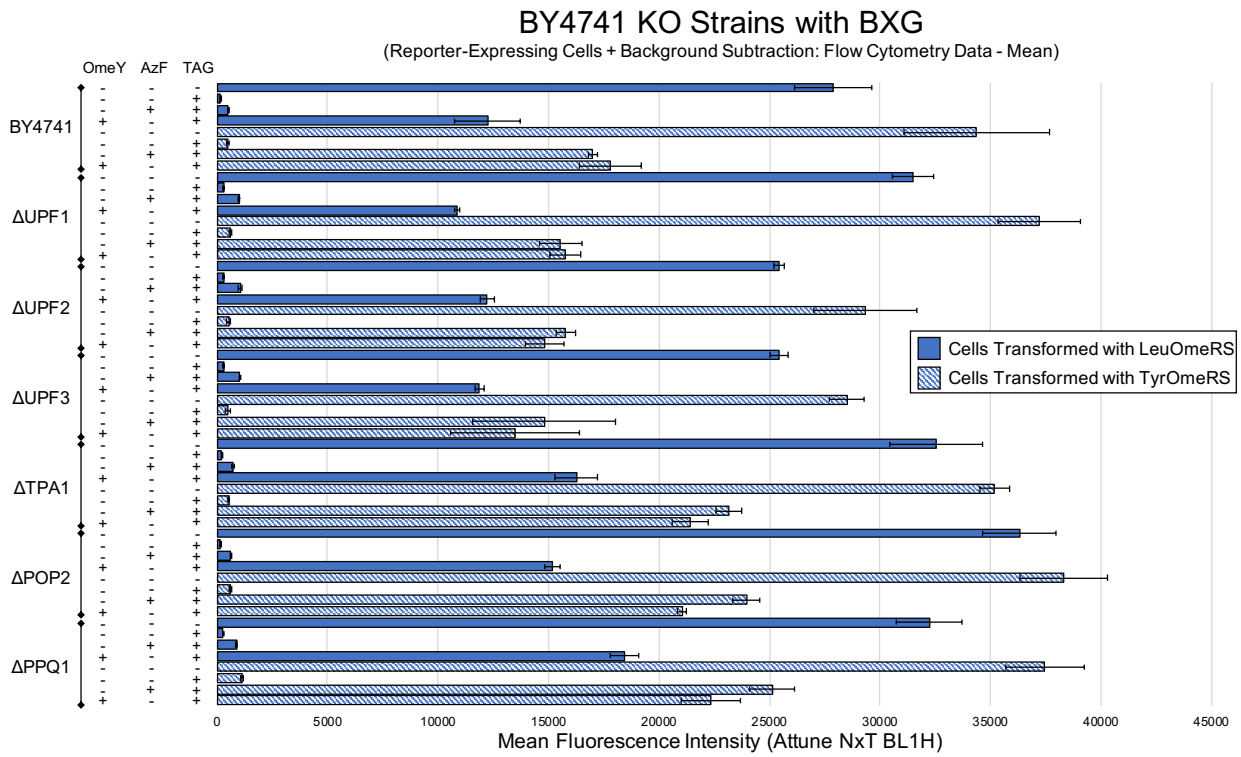

Fig. S26: Alternate analysis of BY4741 and six single-gene knockout strains using the BXG BFP-GFP dual-fluorescent protein reporter. Measurements for the efficiency of ncAA incorporation calculated with mean fluorescence intensity using reporter-expressing cells with background subtraction. The condition denoted by absence of ncAAs and a TAG codon is the wild-type reporter construct induced in the absence of ncAAs.

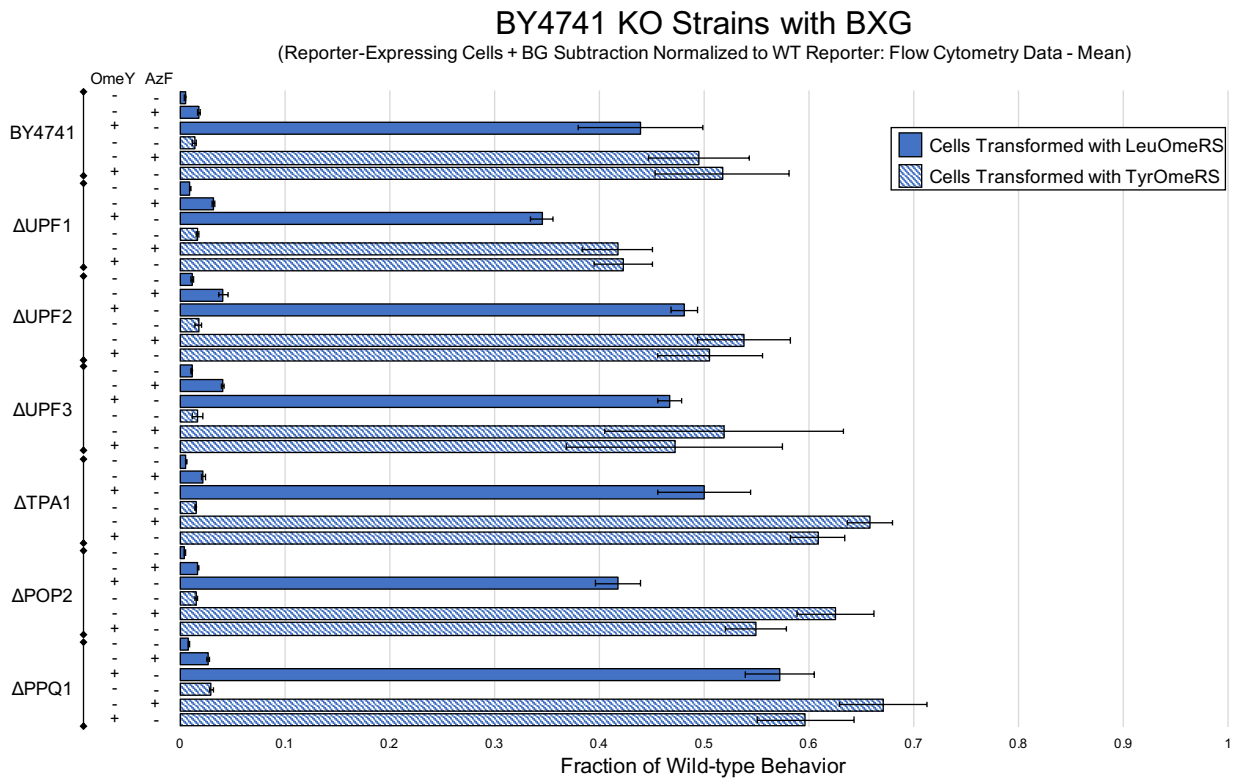

Fig. S27: Alternate analysis of BY4741 and six single-gene knockout strains using the BXG BFP-GFP dual-fluorescent protein reporter. Measurements for the efficiency of ncAA incorporation calculated using the mean fluorescence intensity of reporter-expressing cells with background subtraction and normalized to mean expression levels of cells expressing the wild-type reporter induced in the absence of ncAAs.

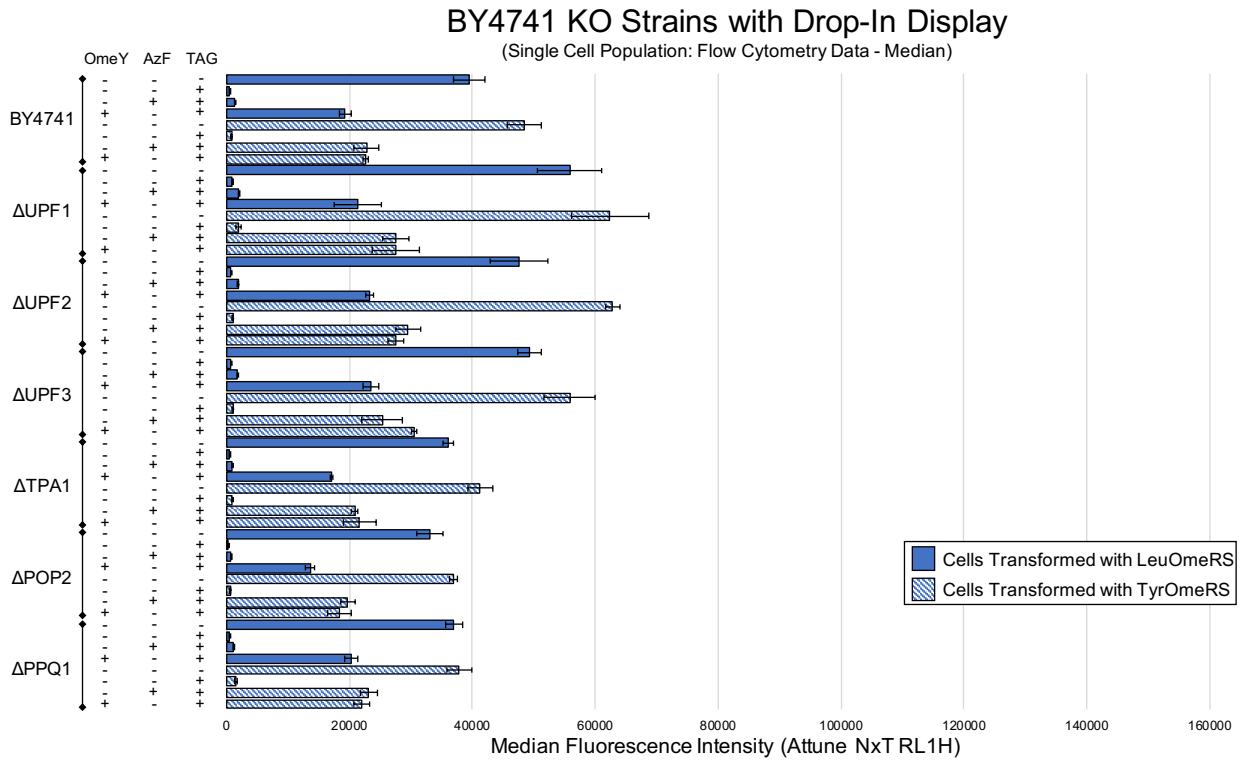

Fig. S28: Alternate analysis of BY4741 and six single-gene knockout strains using the drop-in yeast display reporter. Measurements for the efficiency of ncAA incorporation calculated with median fluorescence intensity using single cell population analysis as described in Materials and Methods Section 2.11. The condition denoted by absence of ncAAs and a TAG codon is the wild-type reporter construct induced in the absence of ncAAs.

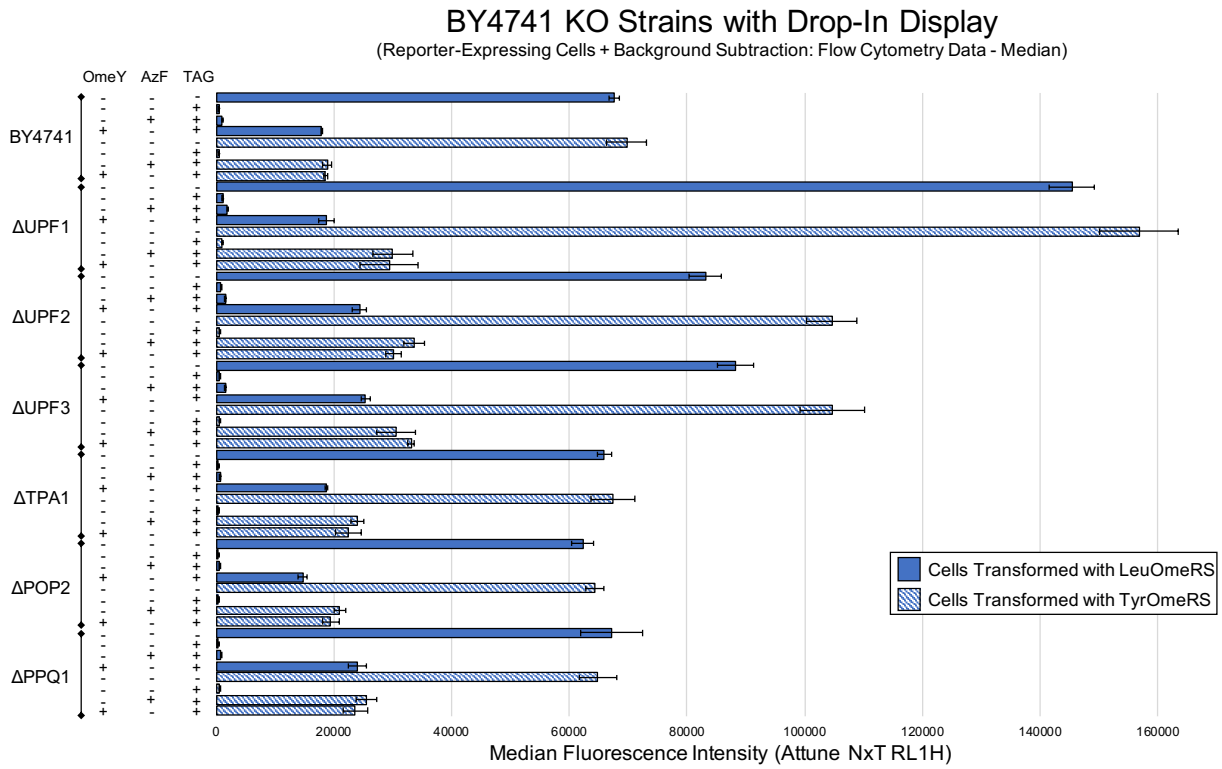

Fig. S29: Alternate analysis of BY4741 and six single-gene knockout strains using the drop-in yeast display reporter. Measurements for the efficiency of ncAA incorporation calculated with median fluorescence intensity of reporter-expressing cells with background subtraction. The condition denoted by absence of ncAAs and a TAG codon is the wild-type reporter construct induced in the absence of ncAAs.

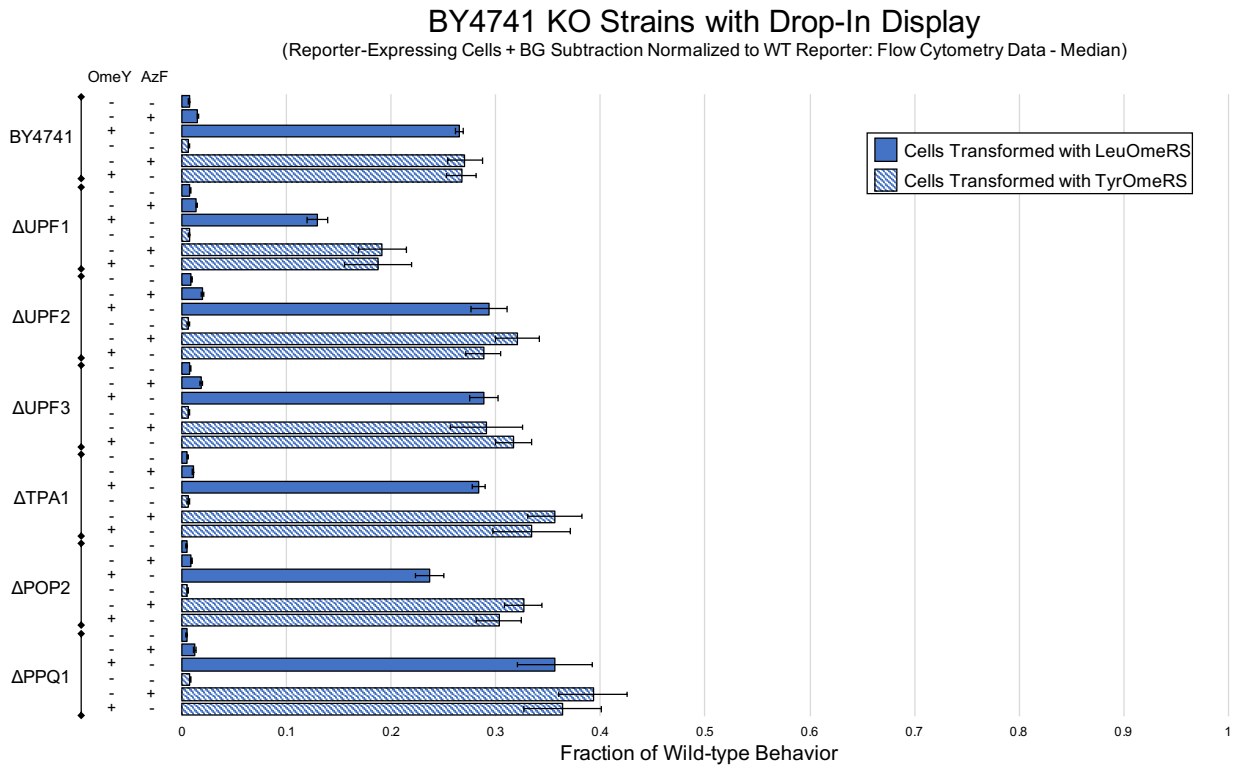

Fig. S30: Alternate analysis of BY4741 and six single-gene knockout strains using the drop-in yeast display reporter. Measurements for the efficiency of ncAA incorporation calculated using the median fluorescence intensity of reporter-expressing cells with background subtraction and normalized to expression levels of cells expressing the wild-type reporter induced in the absence of ncAAs.

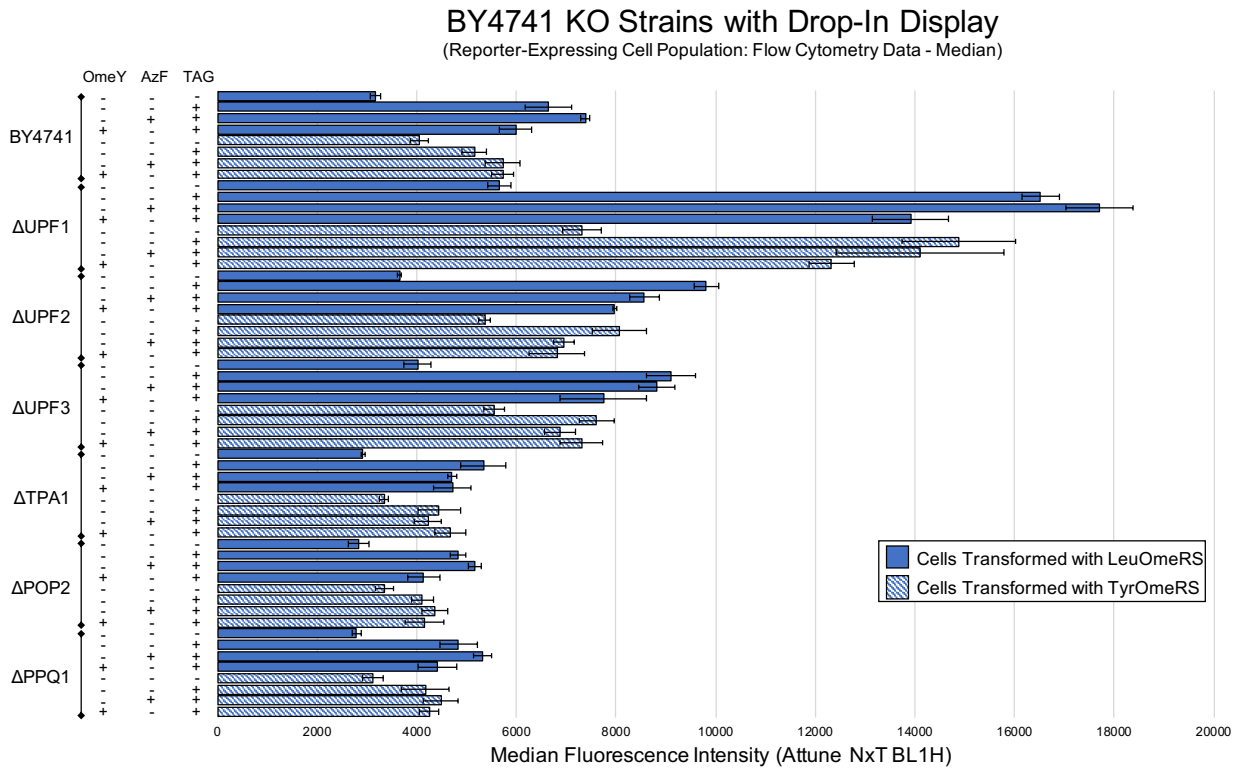

Fig. S31: Measurement of reporter expression level in BY4741 and six single-gene knockout strains containing the drop-in yeast display reporter using the median fluorescence intensity of the cell population exhibiting above-background reporter expression. The condition denoted by absence of ncAAs and a TAG codon is the wild-type reporter construct induced in the absence of ncAAs.

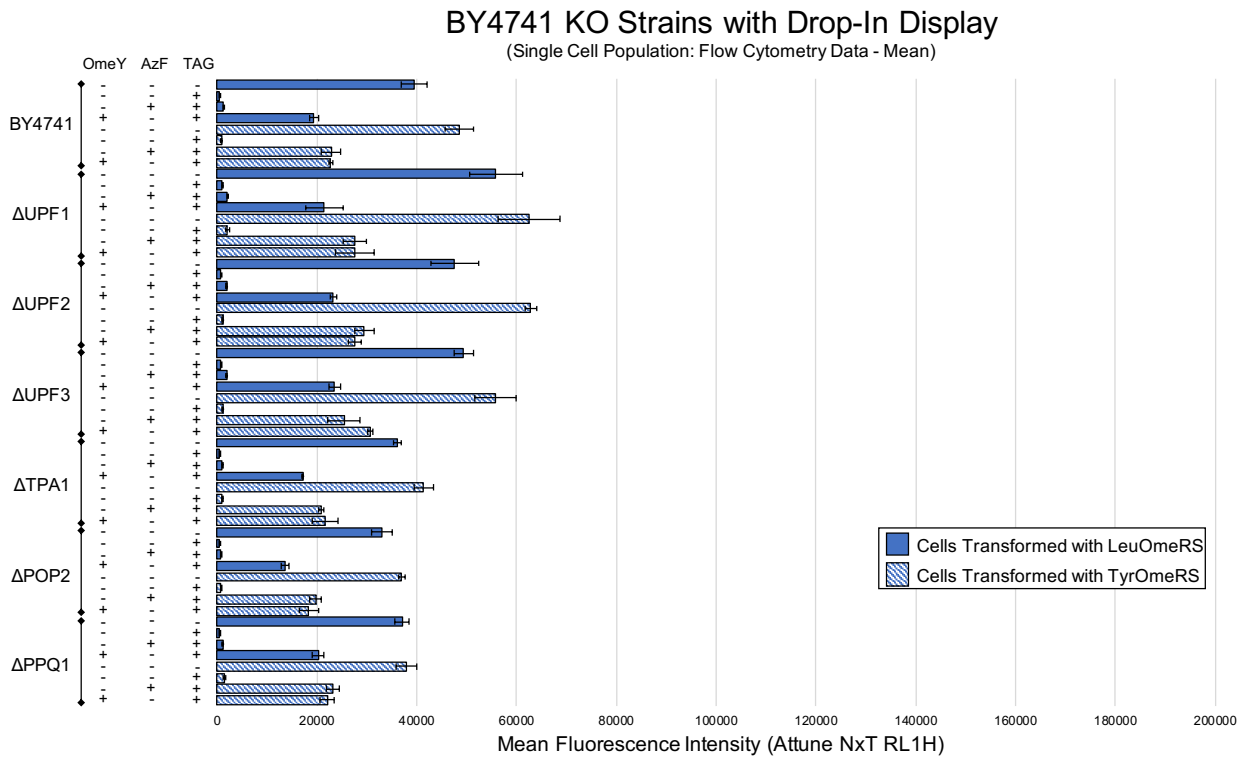

Fig. S32: Alternate analysis of BY4741 and six single-gene knockout strains using the drop-in yeast display reporter. Measurements for the efficiency of ncAA incorporation calculated with mean fluorescence intensity using single cell population analysis. The condition denoted by absence of ncAAs and a TAG codon is the wild-type reporter construct induced in the absence of ncAAs.

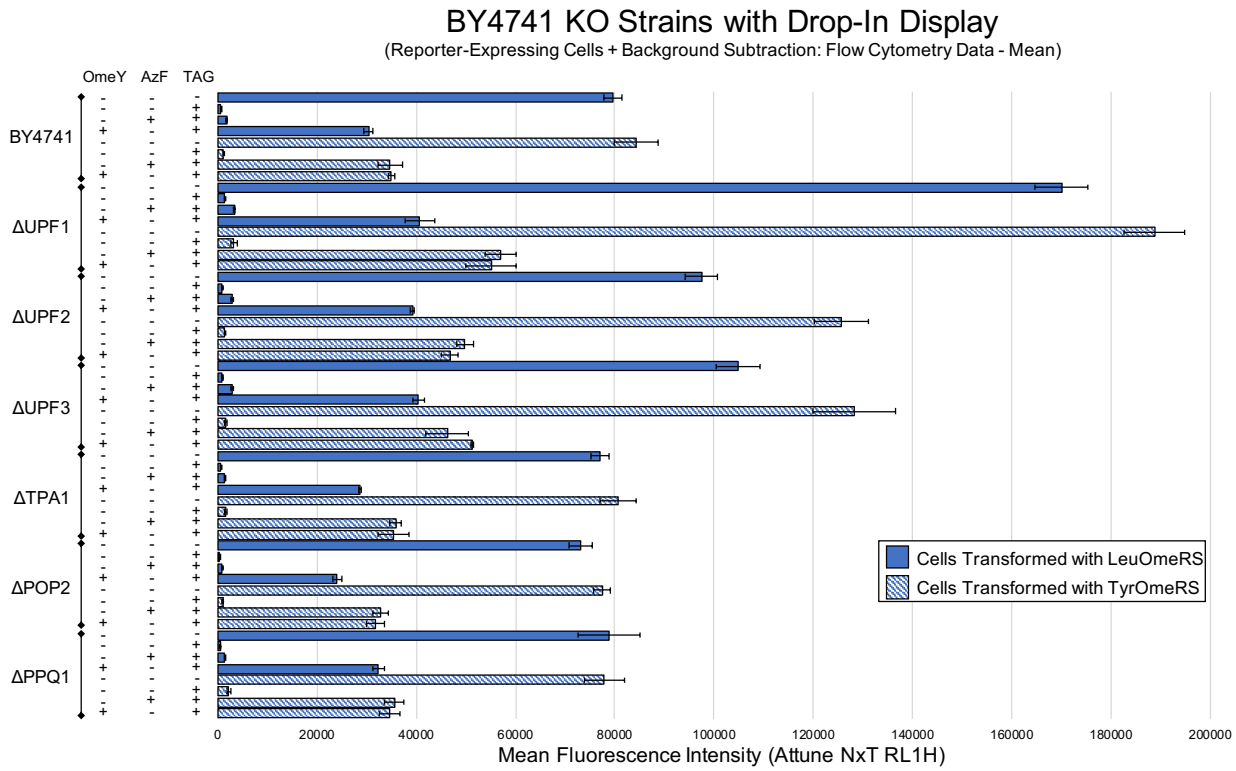

Fig. S33: Alternate analysis of BY4741 and six single-gene knockout strains using the drop-in yeast display reporter. Measurements for the efficiency of ncAA incorporation calculated with mean fluorescence intensity using reporter-expressing cells with background subtraction. The condition denoted by absence of ncAAs and a TAG codon is the wild-type reporter construct induced in the absence of ncAAs.

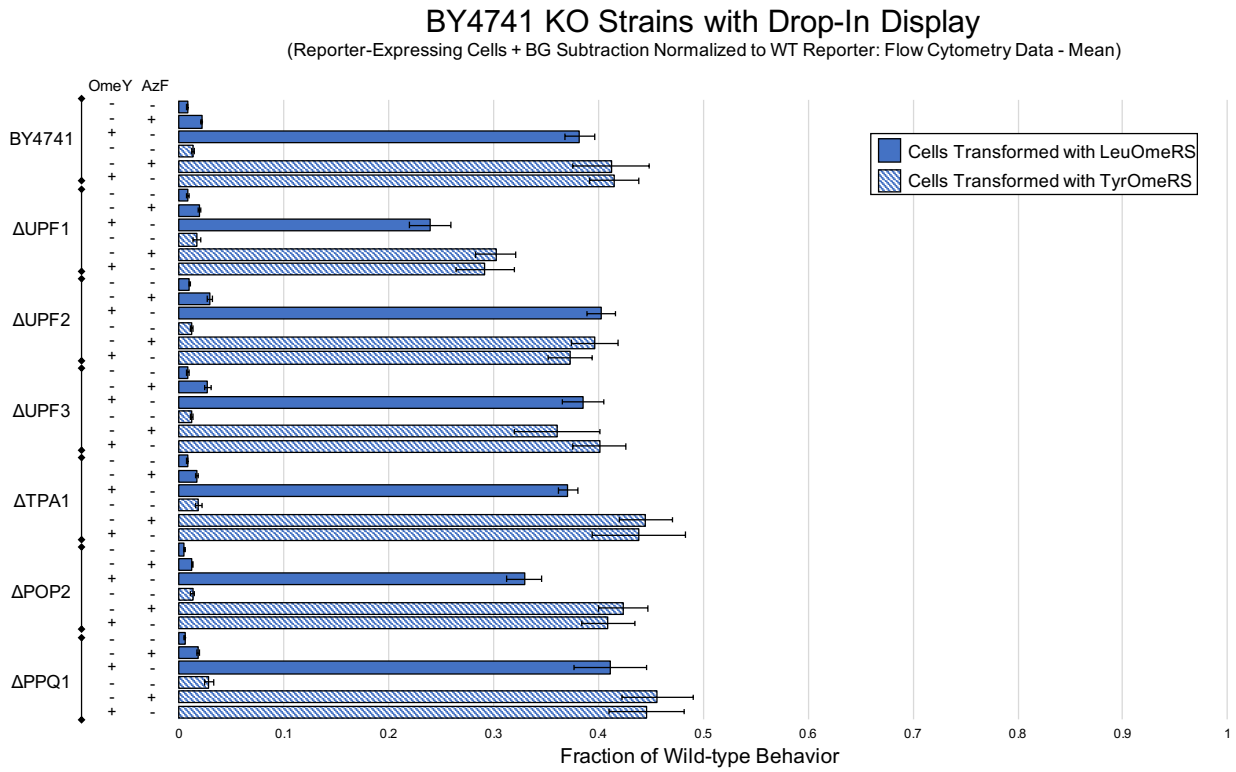

Fig. S34: Alternate analysis of BY4741 and six single-gene knockout strains using the drop-in yeast display reporter. Measurements for the efficiency of ncAA incorporation calculated using the mean fluorescence intensity of reporter-expressing cells with background subtraction and normalized to expression levels of cells expressing the wild-type reporter in the absence of ncAAs.